

博士論文  
(Doctoral Thesis)

Enzyme engineering of phosphite dehydrogenase  
and its applications for biotechnology  
亜リン酸デヒドロゲナーゼの酵素工学的改変と  
バイオテクノロジーへの応用

Gamal Nasser Abdelhady Abdelhamid

広島大学大学院先端物質科学研究科  
[Graduate School of Advanced Sciences of Matter]  
Hiroshima University

2021年9月

(September 2021)

## Table of Contents

### 1. Main Thesis

#### **Enzyme engineering of phosphite dehydrogenase and its applications for biotechnology**

(亜リン酸デヒドロゲナーゼの酵素工学的改変とバイオテクノロジーへの応用)

### 2. Articles

(1) Synthetic phosphorus metabolic pathway for biosafety and contamination management of cyanobacterial cultivation.

Kei Motomura, Kosuke Sano, Satoru Watanabe, Akihiro Kanbara, Gamal Nasser Abdel-Hady, Takeshi Ikeda, Takenori Ishida, Hisakage Funabashi, Akio Kuroda, and Ryuichi Hirota.

ACS Synthetic Biology, **7**, 2189-2198 (2018).

(2) Engineering cofactor specificity of a thermostable phosphite dehydrogenase for a highly efficient and robust NADPH regeneration system.

Gamal Nasser Abdel-Hady, Takeshi Ikeda, Takenori Ishida, Hisakage Funabashi, Akio Kuroda, and Ryuichi Hirota.

Frontiers in Bioengineering and Biotechnology, **9**, 647176 (2021).

# **Main Thesis**

<b>Contents</b>	<b>Page</b>
<b>Chapter 1. General introduction</b>	
1.1 Microbial oxidation of reduced phosphorus compounds .....	2
1.2 Biotechnological applications of phosphite dehydrogenase (PtxD).....	3
1.3 Research purpose of this thesis.....	5
<b>Chapter 2. Biological containment application of RsPtxD for Cyanobacteria</b>	
2.1 Introduction.....	8
2.2 Experimental Section	
2.2.1 Bacterial strains and culture conditions.....	11
2.2.2 Plasmid construction.....	15
2.2.3 Strain construction.....	19
2.2.4 Immunoblot analysis.....	20
2.2.5 Characterization of a Pit homologue from <i>Syn 7942</i> .....	20
2.2.6 Assessment of P availability.....	21
2.2.7 Escape assay and long-term viability.....	22
2.2.8 Growth competition assay.....	22
2.3 Results and Discussion	
2.3.1 Replacement of HtxB Signal peptide for functional expression of the Htx transporter in <i>Syn 7942</i> .....	23
2.3.2 Identification of endogenous Pi transporters in <i>Syn 7942</i> .....	27
2.3.3 Pt-dependent <i>Syn 7942</i> strain construction.....	27
2.3.4 Availability of P sources for strain RH714.....	33
2.3.5 Escape frequency and long-term viability.....	36

2.3.6	Growth competition between RH714 and wild-type cyanobacteria.....	38
-------	---	----

### **Chapter 3. Engineering cofactor specificity of RsPtxD toward NADP**

3.1	Introduction.....	43
3.2	Experimental Section	
3.2.1	RsPtxD mutant's creation using site-directed mutagenesis.....	46
3.2.2	Overexpression and purification of RsPtxD protein .....	48
3.2.3	Enzyme kinetics analysis.....	49
3.2.4	Optimal temperature for RsPtxD proteins.....	49
3.2.5	Thermostability and organic solvents tolerance of RsPtxD mutants.....	50
3.2.6	Optimal pH for RsPtxD proteins.....	50
3.2.7	SA production and detection.....	50
3.3	Results	
3.3.1	Construction of RsPtxD mutants.....	52
3.3.2	RsPtxD mutant's kinetic analysis .....	54
3.3.3	Optimal temperature, thermostability, and organic solvent tolerance of RsPtxD mutants.....	57
3.3.4	The optimal pH of RsPtxD variants.....	61
3.3.5	Production of SA by utilizing RsPtxD as an NADPH generation system.....	61
3.4.	Discussion	
3.4.1	RsPtxD mutants with higher affinity toward NADP.....	62
3.4.2	The optimal pH shift of RsPtxD variants.....	66
3.4.3	Thermostability and solvent stability are improved by higher NADP affinity of RsPtxD variants .....	69

3.4.4 Comparisons with other research studies for cofactor switching and improvements in NADP-regeneration enzymes.....	72
<b>Chapter 4. General conclusions.....</b>	<b>75</b>
<b>References.....</b>	<b>78</b>
<b>Acknowledgments.....</b>	<b>93</b>

# **Chapter 1**

## **General introduction**

## 1.1 Microbial oxidation of Pt and HPt compounds

Phosphorus (P) is an indispensable nutrient for all living organisms due to its crucial role in metabolism. In addition to its participation in numerous metabolic pathways, P is also present in important cellular constituents such as DNA, RNA, phosphoproteins, phospholipids, sugar phosphates, enzymes, and energy-rich phosphorus compounds such as ATP and NADP. In natural environments, all biologically available P is mainly present in the form of inorganic phosphate ( $\text{H}_2\text{PO}_4$ , Pi) in the most oxidized state (P valence of +5) or organic phosphate esters. On the other hand, P-containing compounds rarely exist in a lower oxidation state, such as phosphite ( $\text{H}_3\text{PO}_3$ , Pt: P valence +3) or hypophosphite ( $\text{H}_3\text{PO}_2$ , HPt: P valence +1) (Figure 1.1). Despite the fact that Pi has been considered the only P form that can be utilized directly by all cells for incorporation into biological processes, a limited number of bacteria have evolved mechanisms for importing and metabolizing reduced P compounds, such as Pt or HPt as alternative P sources via oxidizing them to Pi prior to P metabolism.

Several investigations have documented microbial oxidation of reduced P molecules such as HPt and Pt. The Gram-negative soil bacterium *Pseudomonas stutzeri* WM88 is a known example of an organism that can utilize HPt and Pt as growth-support P sources via *htx* and *ptx* operons, respectively (1). HPt uptake and oxidation are offered by the HtxABCDE operon. The *htxBCDE* gene products most likely encode a binding- protein-dependent transporter that selectively uptake HPt and Pt, but not Pi (Figure 1.2). Following uptake, HPt is oxidized to Pt by hypophosphite dioxygenase (HtxA) (2). The produced Pt is subsequently oxidized to Pi by NAD-dependent Pt dehydrogenase (PtxD) (3).

## 1.2 Biotechnological applications of Phosphite dehydrogenase (PtxD)

Pt dehydrogenase (PtxD), which catalyzes the oxidation of Pt to Pi coupling with the reduction of NAD to NADH, was first isolated from *Pseudomonas stutzeri* WM88 (PsePtxD) and considered to have a variety of industrial applications (3). However, PsePtxD exhibited lower thermostability and expressed as an insoluble form in *Escherichia coli*, restricting the practical application of this enzyme (4). Following this discovery, Hirota et al, obtained a highly stable and soluble expressed PtxD from a thermostable soil bacterium *Ralstonia* sp. 4506 (RsPtxD), RsPtxD has a 3,450-fold longer half-life at 45°C (80.5 h) and a 7-fold higher catalytic efficiency than PsePtxD (5). In addition to the unique enzymatic properties of PtxD enzymes, Pt is not used as a P source for most eukaryotes and prokaryotes, and is scarce in natural environments, which offer interesting biotechnology applications; i) highly efficient NADH regeneration system due to the great thermodynamic driving force for Pt-oxidation ( $\Delta G^{\theta} = -15$  kcal/mol), ii) because most organisms are unable to utilize Pt as a sole P source, heterologous expression of PtxD confers a competitive growth advantage of host cells in Pt-containing growth conditions, ensuring contamination management in practical applications (e.g. open ponds, large scale fermentation), and/or iii) developing a biocontainment strategy via engineering the P metabolic pathway for nutrient dependency on Pt for a biosafety measure.

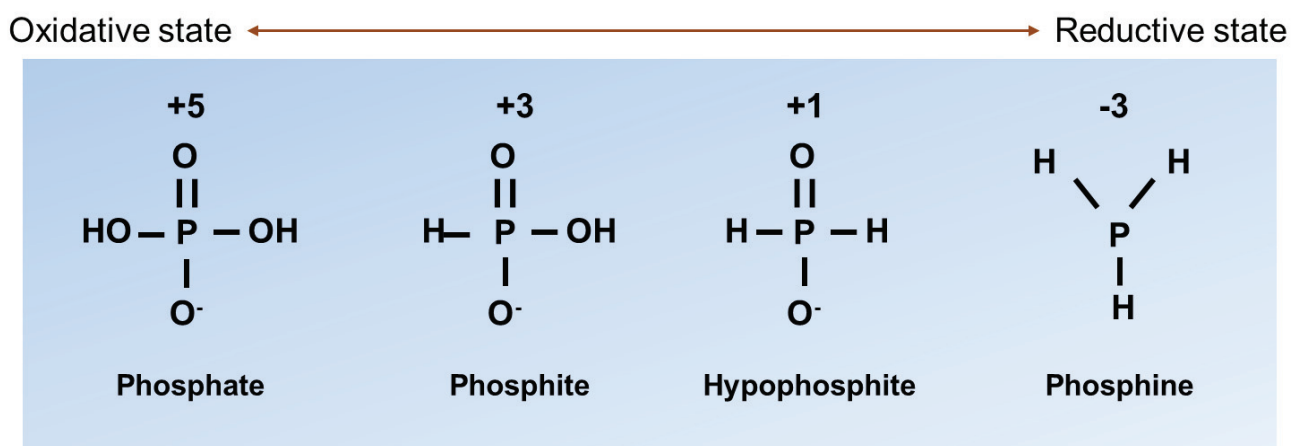


**Figure 1.1** Chemical structure of Phosphate and its reduced forms.

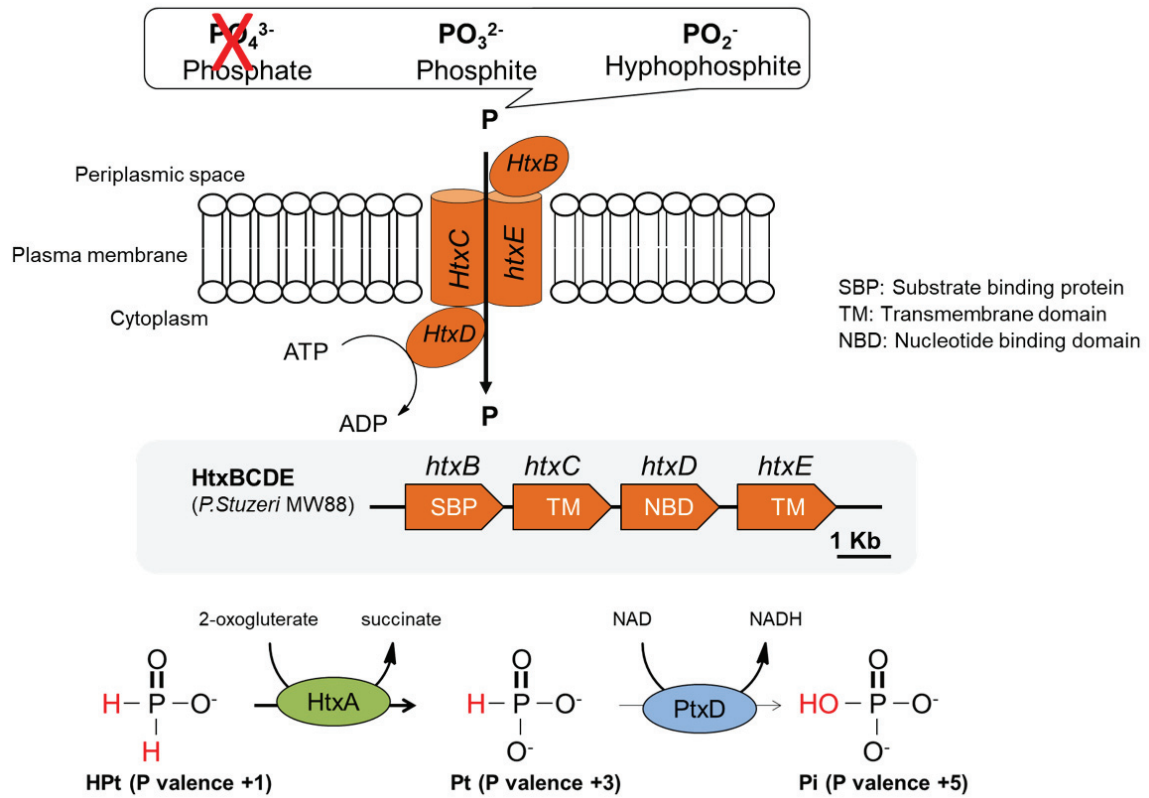


**Figure 1.2** Schematic illustration of phosphite and hypophosphite selective uptake and oxidation. Following uptake across the plasma membrane by the HtxBCDE-transporters, hypophosphite is converted to phosphite by the hypophosphite:2-oxoglutarate dioxygenase, HtxA, and phosphite is oxidized to phosphate by the phosphite dehydrogenase (PtxD).

### 1.3 Research purpose of this study

Although PtxD is potentially useful for developing unique biotechnology applications, the current PtxD enzymes extensively utilize NAD as a cofactor, rendering these applications impractical or less effective. As a result, this study attempted to broaden the biotechnological applications of PtxD isolated from *Ralstonia* sp. 4506 (RsPtxD) by:

- I) Deploying the Pt-dependent biocontainment strategy that has been established in heterotrophic organism *E.coli* to the model cyanobacterium *Synechococcus elongatus* PCC 7942 (Syn 7942) by expressing RsPtxD and HtxBCDE proteins and evaluating its effect.
- II) Engineering RsPtxD's cofactor specificity toward NADP for developing a universal and highly effective NAD(P)H regeneration system.

The first topic is discussed in chapter 2. The author established the biocontainment strategy based on Pt dependency of the model cyanobacterium *Synechococcus elongatus* PCC 7942 which was initially developed in the heterotrophic bacterium *E. coli*. Disruption of all indigenous Pi transporter coupling with exogenous expression of RsPtxD and HtxBCDE transporter that selectively take up Pt but not Pi, makes this genetically engineered strain strictly grow on Pt. Therefore, given the paucity of Pt in aquatic environments, the author confirmed that this strategy contributes to resolving biosafety concerns and controlling the risk of contamination of genetically modified cyanobacteria intended for use outside of enclosed laboratory facilities.

The second topic is discussed in chapter 3. The cofactor specificity of RsPtxD has been engineered for an effective NADPH regeneration system. Site-directed mutagenesis was used to replace five amino acid residues in the Rossmann-fold domain of RsPtxD, resulting in four mutants

with higher NDAP affinity. The generated RsPtxD mutants with a great affinity for NADP, make them a promising alternative NADPH regeneration system for practical applications.

Finally, chapter 4 summarizes the findings and discusses the expected impact of RsPtxD mutants on maintaining the redox balances [NAD(P)H/NAD(P)] at proper levels under the growth of Pt of the genetically modified *Synechococcus elongatus* PCC 7942 as a possible solution for the lower growth of Pt-dependent strain created in chapter 2

## **Chapter 2**

### **Biological containment application of RsPtxD for Cyanobacteria**

## 2.1 Introduction

Recently, cyanobacteria have become attractive owing to their potential biological applications, due to their ability to grow photoautotrophically and produce high-value chemicals (6,7). Furthermore, they have been considered as promising host organisms for sustainable bioproduction due to their ability to utilize CO<sub>2</sub> using sunlight energy, thereby minimizing greenhouse gases and retarding climate changes. Recent advances in genetic and metabolic engineering have enabled cyanobacteria to produce a wide range of biochemicals and biofuels with high productivity (8).

Biodiversity and biosafety are the major concerns for the practical use of engineered cyanobacteria in the open environment. Therefore, they must be cultivated in enclosed bioreactors. However, an open pond system, such as the raceway type, is appropriate for the industrial cultivation of microalgae, including cyanobacteria, because it is easy and requires less energy for operational procedures (9). As a result, safeguarding methods to prevent the undesired outgrowth of engineered cyanobacteria need to be established before implementing cyanobacteria in practical applications. Open pond cultivation is also always subjected to the risk of contamination, which impairs the culture of the desired microalgae (ideally a monoculture) and lowers productivity. Genetic engineering based-strategies have been suggested to alleviate the impact of contamination (10), but none of the genetically modified strains can be used in open environments due to biosafety concerns (11).

Biocontainment is a methodology for safeguarding against the uncontrolled spread of genetically modified microorganisms (12). Basically, it can be categorized based on the restraint mechanism. Active containment approaches utilize controllable kill switches that bring about cell death; these contain toxin and antitoxin gene pairs (13,14), and proteins that damage self DNA

(15,16). Passive containment approaches are intended to produce cells that are dependent on external additives, by disrupting the function of specific genes. This method generates microorganisms that require externally added chemicals for their growth. Recent studies have revealed that strict dependence on the availability of non-standard amino acids (17,18) and a synthetic chemical (19) for growth yields a high containment efficacy. In the natural environment, the modified strains fail to survive due to the absence of such synthetic compounds.

Phosphorus (P), a component of nucleic acids, lipids, and a variety of cellular metabolites, is an indispensable nutrient for all living organisms. Naturally, all biologically available P is in the form of phosphate ( $\text{H}_3\text{PO}_4$ , Pi) and its esters. However, a limited number of bacteria can utilize other reduced P compounds such as phosphite ( $\text{H}_3\text{PO}_3$ , Pt) and hypophosphite ( $\text{H}_3\text{PO}_2$ , HPt), taking up and oxidizing these reduced P compounds. The mechanisms for metabolizing Pt and HPt have been established in the soil bacterium *Pseudomonas stutzeri* WM88, which possesses *htx* and *ptx* operons for assimilating HPt and Pt, respectively (1). HPt is taken up via the HtxBCDE transporter and oxidized to Pt by HPt dioxygenase (HtxA) (2). The resultant Pt is then oxidized to Pi by the NAD-dependent Pt dehydrogenase (PtxD) (3). Although recent research has been suggested the presence of a biological P redox cycle in nature (20), HPt and Pt are rarely detected in the environment (21,22).

Reduced P assimilation pathways offer new biotechnological applications for controlling the growth of host organisms and contaminants by managing their P availability (23). Heterologous expression of *ptxD* provides host cells, such as bacteria (24), yeast (23), and microalgae with a competitive growth advantage over contaminating organisms by broadening their range of metabolizable P substrates. For most contaminating organisms, Pt is a nonmetabolizable form of P; only *ptxD*-transformed cells could thrive on media containing Pt as

the sole P source (23-26). Because Pt is inexpensive, this allows selective cultivation suitable for large-scale fermentation processes (26). Furthermore, based on the rarity of Pt in the environment, Hirota et al., recently established a novel biocontainment strategy for *E. coli* using engineered nutrient dependency on Pt (27). Endogenous Pi compound transporters were disrupted in a PtxD-harboring *E. coli* strain that expresses HtxBCDE, a transporter that selectively takes up Pt but not Pi, which resulted in a strict growth dependency on Pt. The genetic modification for this P metabolic engineering is easy, and results in a high level of containment efficacy, suggesting that the strategy is reliable and may be extensively employed. As a result, modified P metabolic pathways can provide two distinct benefits: “biological containment” and “contamination management”, both of which are necessary to solve the abovementioned challenges in microalgal cultivation for practical scenario. A growing number of biological containment approaches have been suggested in recent years, but none of them, as far as we know, have the effect of also reducing contamination concerns.

In the current study, the P metabolic pathway of the model cyanobacterium *Synechococcus elongatus* PCC 7942 (hereafter called *Syn* 7942) has been engineered to make it Pt-dependent. The modified Pt-dependent strain exhibited strict growth on Pt, extremely low escape frequency, and quick loss of viability in the absence of Pt, like the study utilizing *E. coli* as the host organism. Furthermore, in a growth medium containing Pt as the P source, the Pt-dependent biocontainment efficiently outcompeted the wild-type cyanobacteria. Considering these properties of the Pt-dependent strain, this strategy helps to ensure biosafety and the risk of contamination management, which opens the way for the application of genetically modified cyanobacteria in outdoor cultivation.

## 2.2 Experimental Section

### 2.2.1 Bacterial strains and culture conditions

The bacteria used in this study are listed in Table 2.1. The wild-type *Syn* 7942 and its derivative strains were routinely cultured at 30 °C with shaking or 2% CO<sub>2</sub> bubbling under continuous illumination (50 μmol photons/m<sup>2</sup>/s) in modified BG11 medium containing 35 mM NaNO<sub>3</sub> (28) (herein referred to as BG11 medium). To make solid media, 20 mM *N*-Tris(hydroxymethyl)-methyl-2-aminoethanesulfonic acid (TES)-KOH (pH 8.0), 1 mM sodium thiosulfate (STS), and 0.75% agar were added to the BG11 medium. Pi contamination in the agar powders was removed by repeated washing with ultrapure deionized water. In experiments with strain RH714, TES buffer and STS were also added to the liquid medium to accelerate cell growth. BG11 media containing 0.2 mM Pi and Pt as the sole sources of P are designated BG11-Pi and BG11-Pt media, respectively. Pt stock solution (1.0 M) was prepared as previously described (27). For supplementation of potassium ions, 0.35 mM KCl was added to BG11-Pt medium. BG11 medium lacking any source of P is designated BG11-0. For P availability assays, different types of P sources including G6P (Sigma-Aldrich, St Louis, MO), ATP (MP Biomedicals, Santa Ana, CA), PPi (Nacalai Tesque, Kyoto, Japan), salmon sperm DNA (Wako, Osaka, Japan), 2-aminoethylphosphonic acid (AEPn; Wako), or methylphosphonic acid (MPn; Sigma-Aldrich) were added to BG11 medium. BG11 media containing P sources derived from aquatic environments were prepared using sterilized waters sampled from a local pond (Budou Pond at Hiroshima University, Hiroshima, Japan) and river (Kurose River, Hiroshima, Japan) instead of distilled water. Pi concentrations in the aquatic samples were determined by the malachite green method (MicroMolar Phosphate Assay Kit; ProFoldin, Hudson, MA). Total P contents was measured as Pi after ammonium persulfate digestion at 121 °C for 30 min (29). To induce the

expression of *htxBCDE* and *ptxD* in *Syn 7942*, 1 mM isopropyl- $\beta$ -D-thiogalactopyranoside (IPTG) was added to the culture media. *E. coli* DH5 $\alpha$  was used as a host for cloning and was grown in 2 $\times$  yeast extract-tryptone (YT) medium (57) at 37 °C. Routine cultivation of *E. coli* MT2012-*ptxD* (27), the Pi transporter-null mutant expressing PtxD, was conducted at 37 °C in modified 2 $\times$  YT medium containing 4% (w/v) yeast extract (double the amount used in the conventional 2 $\times$  YT medium). When necessary, spectinomycin (40  $\mu$ g/mL for *Syn 7942*), gentamicin (2  $\mu$ g/mL for *Syn 7942*), kanamycin (10  $\mu$ g/mL for *Syn 7942*),

**Table 2.1.** Bacterial strains used in this study

Strain	Genotype or relevant characteristics <sup>a</sup>	Source or
<b><i>Synechococcus elongatus</i> strains</b>		
PCC 7942  (herein <i>Syn</i> 7942)	Wild-type strain	Laboratory stock
RH683	NS1:: <i>htxBCDE-ptxD</i>	This study
RH693	NS1:: <i>htxBCDE</i> <sub>7120-SP</sub> - <i>ptxD</i>	This study
RH696	NS1:: <i>htxBCDE</i> <sub>Ral-SP</sub> - <i>ptxD</i>	This study
RH697	NS1:: <i>htxBCDE</i> <sub>Syn-SP</sub> - <i>ptxD</i>	This study
RH713	NS1:: <i>htxBCDE</i> <sub>7120-SP</sub> - <i>ptxD</i> $\Delta$ <i>pit</i> ::Gm <sup>R</sup>	This study
RH714	NS1:: <i>htxBCDE</i> <sub>7120-SP</sub> - <i>ptxD</i> $\Delta$ <i>pit</i> ::Gm <sup>R</sup> <i>ΔsphX-pstSCAB</i> ::Km <sup>R</sup> , clone 1	This study
RH715	NS1:: <i>htxBCDE</i> <sub>7120-SP</sub> - <i>ptxD</i> $\Delta$ <i>pit</i> ::Gm <sup>R</sup> <i>ΔsphX-pstSCAB</i> ::Km <sup>R</sup> , clone 2	This study
RH716	NS1:: <i>htxBCDE</i> <sub>7120-SP</sub> - <i>ptxD</i> $\Delta$ <i>pit</i> ::Gm <sup>R</sup> <i>ΔsphX-pstSCAB</i> ::Km <sup>R</sup> , clone 3	This study

## Others

<i>Escherichia coli</i> DH5 $\alpha$	Cloning host strain	Commercially available
<i>E. coli</i> MG1655	Source of <i>pitA</i> gene	Laboratory stock
<i>E. coli</i> MT2012- <i>ptxD</i>	Pi transporter-null mutant expressing PtxD from <i>Ralstonia</i> sp. 4506	(27)
<i>Anabaena</i> sp. PCC 7120 (herein <i>Ana</i> 7120)	Source of signal peptide sequence, harboring <i>ptxABCD</i> gene	Laboratory stock
<i>Ralstonia</i> sp. 4506	Source of signal peptide sequence, harboring <i>ptxABCD</i> gene	(5)

---

<sup>a</sup> Gm<sup>R</sup>, gentamicin resistance; Km<sup>R</sup>, kanamycin resistance.

carbenicillin (50 µg/mL for *E. coli*), and chloramphenicol (30 µg/mL for *E. coli*) were added to the appropriate medium.

### 2.2.2 Plasmid construction

The plasmids used in this study are listed in Table 2.2. The plasmid carrying *P. stutzeri* WM88 *htxBCDE* was amplified by reverse PCR using pSTVhtxAE (27) as the template with primers htx-IF1 and htx-IR1 (Table 2.3). The amplified fragment was self-ligated to yield pSTVhtxBE. For the construction of pNSptxAD, a DNA fragment containing the *ptxABCD* operon was amplified by PCR from genomic DNA of *Ralstonia* sp. 4506 (27) using the primer pair ptx-F1 and ptx-R1. The resultant fragment was inserted into the *EcoRI/HindIII* sites of pNSHA using the In-Fusion HD cloning kit (Takara Bio, Tokyo, Japan). To construct plasmids carrying *htxBCDE* transcriptionally fused to *ptxD*, a DNA fragment containing *htxBCDE* was amplified by PCR using pSTVhtxBE as the template with primers htx-F1/htx-R1, and cloned into pNSptxAD digested with *EcoRI* and *SalI* using the In-Fusion reaction, yielding pNShtxBE-ptxD. For evaluating the compatibilities of the SP sequences of HtxB, DNA fragments containing the SPs of *Ana* 7120 PtxB (30), *Ralstonia* sp. 4506 PtxB (27), and *Syn* 7942 PstS (31) were amplified by PCR using primer pairs Anaptx-F/Anaptx-R, Ralptx-F/Ralptx-R, and Synpst-F/Synpst-R, respectively. The amplified fragments were inserted using the In-Fusion kit into pSTVhtxBE that had been linearized by reverse PCR with primers htx-IF2 and htx-IR2. The resulting plasmids were used as templates for amplifying the *htx* operons including the modified *htxBs* with primers htx-F2/htx-R1, following which the amplified fragments were introduced into pNSptxAD digested with *EcoRI/SalI* by the In-Fusion method, to yield pNShtxBE<sub>7120-SP</sub>-ptxD, pNShtxBE<sub>Ral-SP</sub>-ptxD, and pNShtxBE<sub>Syn-SP</sub>-ptxD, respectively. All the DNA fragments cloned into plasmids were verified by sequencing.

**Table 2.2** Plasmids used in this study

Plasmid	Genotype or relevant characteristics <sup>a</sup>	Source or
pSTV28	Cloning vector; Cm <sup>R</sup>	Takara Bio
pSTVhtxAE	pSTV28 carrying <i>htxABCDE</i>	(27)
pSTVhtxBE	pSTV28 carrying <i>htxBCDE</i>	This study
pSTVhtxBE <sub>7120-SP</sub>	pSTV28 carrying modified <i>htxBCDE</i> ; HtxB signal peptide is replaced with that	This study
pSTVhtxBE <sub>Ral-SP</sub>	pSTV28 carrying modified <i>htxBCDE</i> ; HtxB signal peptide is replaced with that	This study
pSTVhtxBE <sub>Syn-SP</sub>	pSTV28 carrying modified <i>htxBCDE</i> ; HtxB signal peptide is replaced with that	This study
pNSHA	Integration vector; Sp <sup>R</sup> in <i>Syn 7942</i>	(56)
pNSptxAD	pNSHA carrying <i>ptxABCD</i> from	This study
pNShtxBE-ptxD	<i>Ralstonia</i> sp. 4506 pNSHA carrying <i>htxBCDE</i> and <i>ptxD</i>	This study
pNShtxBE <sub>7120-SP</sub> -ptxD	pNSHA carrying modified <i>htxBCDE</i> (HtxB <sub>7120-SP</sub> ) and <i>ptxD</i>	This study
pNShtxBE <sub>Ral-SP</sub> -ptxD	pNSHA carrying modified <i>htxBCDE</i> (HtxB <sub>Ral-SP</sub> ) and <i>ptxD</i>	This study
pNShtxBE <sub>Syn-SP</sub> -ptxD	pNSHA carrying modified <i>htxBCDE</i> (HtxB <sub>Syn-SP</sub> ) and <i>ptxD</i>	This study
pMW118	Cloning vector; Amp <sup>R</sup> , a pSC101	Nippon Gene
pMW119	derivative low-copy-number vector Cloning vector; Amp <sup>R</sup> , a pSC101	Nippon Gene
pMWpitA <sub>Eco</sub>	pMW118 carrying <i>E. coli</i> MG1655 <i>pitA</i>	This study
pMWpitA <sub>Syn</sub>	pMW119 carrying <i>Syn 7942</i> <i>pit</i>	This study

<sup>a</sup> Cm<sup>R</sup>, chloramphenicol resistance; Sp<sup>R</sup>, spectinomycin resistance; Amp<sup>R</sup>, ampicillin resistance.

**Table 2.3** DNA primers used in this study

Primer	Sequence (5' to 3') <sup>a</sup>
<b>Plasmid construction</b>	
htx-IF1	ATGCAAGTTTTTACTCTGTTTTTCG
htx-IR1	GGTGATGCTCCTAGGATCCCCG
ptx-F1	acagaccatggaattCGTGTCATATCACGACATTACCATCG
ptx-R1	caaaacagccaagctTTCACGCCGCTTTACTCCCGGATAC
htx-F1	acagaccatggaattCATGCAAGTTTTTACTCTGTT
htx-R1	agctgaaggcgtcgaCTAGTAGTTGCGGGCCGCGA
Anaptx-F	cctaggagcatcaccatgGCGATCGCAATC
Anaptx-R	attgacaacctcagcAGCTGCGCTCTTTGC
Ralptx-F	cctaggagcatcaccatgAAAAAACTCGCATC
Ralptx-R	attgacaacctcagcGGATGATGCATGGCC
Synpst-F	cctaggagcatcaccatgGCTTCCCTAAAATTCC
Synpst-R	attgacaacctcagcACCAGAGCTGCAAGC
htx-IF2	CATGGTGATGCTCCTAGGATCCCCG
htx-IR2	GCTGAGGTTGTCAATGGTAAACTTC
htx-F2	acagaccatggaattCATCCTAGGAGCATCACCATG
Synpit-F	cacaaggagactgccATGATCGCGGCCTTACTGGAAC
Synpit-R	tggcagtttatggcgTCAGGCCCAAATCGCACGCC
EcopitA-F	<u>AAGAATTC</u> ATGCTACATTTGTTTGCTGGC
EcopitA-R	AAAT <u>CCTAGATT</u> ACAGGAACTGCAAGGAGAG
<b>Mutant construction</b>	
pit-uF	CCGGTGCGAGATGTTTCAGCG
pit-uR	GCGTCACCCGGCAATCATGAGCGAGGCGGCAAGGACT
pit-dF	GTACCGCCACCTAATGCTCACCGTTGTTGTCAGG
pit-dR	ACCTGTCAGAAATTGGCGATCGAT
gmr-F	GCCGCCTCGCTCATGATTGCCGGGTGACGCACACCGTGGAAA
gmr-R	CAACAACGGTGAGCATTAGGTGGCGGTACTTGGGTC
pst-uF	GGCGGACATTGCCGACGCCAACGCGGG
pst-uR	CGCTCACAATTCCACTTAGACTTTGGTGCGATCGGTA
pst-dF	GATGAGTTTTTCTAAACCCTGAAGCCATCACCCTTT

pst-dR	GCCCATCGAGGTGGAGCCGTTGG
kmr-F	TCGCACCAAAGTCTAAGTGG AATTGTGAGCGGATAACAAT
kmr-R	GTGATGGCTTCAGGGGTTTAGAAAACTCATCGAGCATCAAATGA

**Mutation confirmation**

NS1-5ex	TTTGAGCGATCGCCAAGCCCAAG
NS1-3ex	AGTTGGCTATCGCTTGGTCAAGG
htx-in	ATGTGGCCACCCGCCATCGC
pit-in	CCCTGACTTGGCCAACCCGTAG
pit-ex	CATTGGAAGTGGTGAGGCTGGCAG
Gm-in	CTCTATACAAAGTTGGGCATACGGG
pst-in	ACTACGTCAGTGGCCGTTTCGGC
pst-ex	TACTCATCGCCTTCGCGGATCAG
Km-in	GCAGTTTCATTTGATGCTCGATGAG
lexA-F	CCTCTACCCGAGCCCAAAA
lexA-R	GGGCCTTTGTTGTTGGAGGC

---

<sup>a</sup> Underlined sequences indicate restriction sites. Lowercase letters represent sequences required for In-Fusion cloning reaction.

### 2.2.3 Strain construction

To obtain *Syn* 7942 strains expressing HtxBCDE and PtxD, the pNSHA-based plasmids carrying the *htxBCDE-ptxD* cassette (pNShtxBE-ptxD, pNShtxBE<sub>7120-SP</sub>-ptxD, pNShtxBE<sub>Ral-SP</sub>-ptxD, and pNShtxBE<sub>Syn-SP</sub>-ptxD) were individually introduced into the wild-type strain via natural transformation. The expression cassettes were integrated into the NS1 of the genome, and the transformants were screened on plates containing spectinomycin to yield strains RH683, RH693, RH696, and RH697. The correct integration of each cassette was confirmed by PCR using primers NS1-5ex, NS1-3ex, and htx-in.

Deletion mutants of the *pit* (Synpcc7942\_0184) and *sphX-pstSCAB* (Synpcc7942\_2441 to 2445) genes were constructed by the allelic replacement method of Kobayashi et al., with slight modifications (32). DNA fragments corresponding to the upstream and downstream regions of *pit* (1 kb each) were amplified by PCR from the chromosomal DNA of *Syn* 7942 using primer sets pit-uF/pit-uR and pit-dF/pit-dR, respectively. The gentamicin resistance gene ( $Gm^R$ ) cassette was amplified by PCR with primers gmr-F and gmr-R. Overlap-extension PCR was performed to assemble these three fragments using primers pit-uF and pit-dR, following which the resulting fragment was introduced into strain RH693 by natural transformation. The transformant colonies were repeatedly streaked onto gentamicin-containing plates to achieve complete segregation, yielding strain RH713. To disrupt the *sphX-pstSCAB* operon, a DNA fragment containing the kanamycin-resistance gene ( $Km^R$ ) cassette was prepared by the same method with primers pst-uF/pst-uR and pst-dF/pst-dR for amplifying the upstream and downstream regions (1.5 kb each) of the operon, respectively, and the primers kmr-F/kmr-R were used to amplify the  $Km^R$  cassette. The resulting fragment was introduced into strain RH713 to generate strains RH714 to RH716.

The complete disruption of the *pit* gene and the *sphX-pstSCAB* operon were confirmed by PCR using the primers pit-in/pit-ex/Gm-in and pst-in/pst-ex/Km-in, respectively (Figure 2.4).

#### **2.2.4 Immunoblot analysis**

Cell cultures at mid-log phase were pelleted, resuspended in cold phosphate-buffered saline (PBS) (0.1 M sodium phosphate and 0.15 M of sodium chloride, pH7.2), and transferred to 2 mL tubes containing lysing matrix B (MP Bio Japan, Tokyo, Japan). The tubes were shaken by a FastPrep bead beater at 4,500 rpm for two cycles of 30 s (MP Bio Japan, Tokyo, Japan). After centrifugation (15,000 rpm for 15 min, 4°C), supernatants were corrected, and protein concentrations were determined by Bio-Rad protein assay using BSA as a standard (Bio-Rad Laboratories Inc. CA, USA). The proteins were then separated by SDS-PAGE, transferred to PVDF membranes, and the membranes were blocked with 2% (wt/vol) of non-fat dry milk in PBS-T (PBS containing 0.05% Tween 20). The membranes were incubated with appropriate antibodies: anti-HtxB (affinity-purified rabbit antibody raised against a synthetic peptide of HtxB (aa 280-292: AKHSDYKVIEDAG) and anti-RbcL (Agrisera, Vännäs, Sweden) at a 1:500 and 1:2,000 dilutions, respectively. After the membranes were washed three times with PBS-T, they were incubated with HRP-conjugated anti-rabbit IgG at a 1:2000 dilution and the immune reactive bands were detected with Eazy West Blue (Atto Corporation, Tokyo, Japan).

#### **2.2.5 Characterization of a Pit homologue from *Syn 7942***

The *pit* homologue from *Syn 7942* (Synpcc7942\_0184) and the *pitA* gene of *E. coli* MG1655 were individually amplified from genomic DNA by PCR using the primer pairs Synpit-F/Synpit-R and EcopitA-F/EcopitA-R (Table 2.3), respectively. The fragments were cloned into the appropriate sites of low-copy-number vectors, following which the resultant plasmids,

pMWpitA<sub>Eco</sub> and pMWpit<sub>Syn</sub>, were introduced into MT2012-*ptxD*. The transformants grown in 2× YT medium were collected in the late log phase by centrifugation and washed thrice with a MOPS-minimal medium containing no P sources (58). The cells were resuspended and diluted in the same medium to an optical density of 1.0 at 600 nm (OD<sub>600</sub>) and inoculated (1%) into fresh MOPS medium containing either 1.0 mM Pi (MOPS-Pi) or Pt (MOPS-Pt). The cultures were incubated at 37 °C with shaking (160 rpm), and the cell growth was automatically recorded every hour using an OD monitoring system (OD-Monitor C&T; TAITEC, Saitama, Japan).

### 2.2.6 Assessment of P availability

The wild-type *Syn* 7942 and RH714 strains were precultured until the OD<sub>750</sub> reached 3.0–5.0 in BG11-Pi and BG11-Pt media, respectively. The cells were centrifuged, washed with an equal volume of BG11-0, and resuspended in the same medium. The suspensions were diluted to an OD<sub>750</sub> of 1.0 and inoculated (1%) into BG11 media containing 0.2 mM Pi, 0.2 mM Pt, 0.2 mM G6P, 67 μM ATP, 0.1 mM PPi, 67 μg/mL salmon sperm DNA, 0.2 mM AEPn, or 0.2 mM MPn. The concentrations of each of the added P sources were adjusted to be equivalent to 0.2 mM Pi. The cells were also inoculated into BG11 media containing P sources from two aquatic environments (Budou Pond and Kurose River), with or without supplementation of 0.2 mM Pi. The pond water (PW) medium contained phosphorus compounds at a concentration of 3.4 μM, although the net Pi concentration was below the detection limit (<0.2 μM). The river water (RW) medium contained 6.4 μM of phosphorus compounds including 4.3 μM Pi. The cultures in 6-well plates were incubated at 30 °C with shaking, and the growth was monitored for 7 days.

### **2.2.7 Escape assay and long-term viability**

For assaying the escape frequency, RH714 cells grown in 25 mL BG11-Pt medium to mid-log phase were centrifuged, washed thrice with 5 mL BG11-0, and resuspended in 10 mL BG11-0. The suspension was spread onto five square plastic dishes (Thermo Fisher Scientific, Kanagawa, Japan) containing BG11-Pi agar media with 0.1 mM IPTG, and colony formation during incubation at 30 °C was monitored for 28 days. To measure the total number of cells used for the assay, aliquots of the suspensions serially diluted with BG11-0 were plated onto BG11-Pt agar medium, and the colonies were counted after incubation at 30 °C for 10 days. The detection limit was calculated as one divided by the total number of CFU plated. To investigate the long-term viability of RH714, 40 mL of cells in late-log phase growing in BG11-Pt medium were pelleted, washed thrice with 10 mL BG11-0, and suspended in the same volume of BG11-0. The suspension was inoculated at an OD<sub>750</sub> of 0.8 into 50 mL of BG11-Pt or -Pi medium. Cultures that were sampled every 2 days were diluted with BG11-0 and spread onto BG11-Pt agar medium, and colony formation was monitored for 10 days.

### **2.2.8 Growth competition assay**

The RH714 and wild-type strains of *Syn* 7942 and *Syn* 6803 precultured until mid-log phase were centrifuged, washed with an equal volume of BG11-0, and resuspended in the same medium. The cell suspensions of RH714, *Syn* 7942, and *Syn* 6803 were diluted to an OD<sub>750</sub> of 0.01, 0.05 and 0.05, respectively, and simultaneously inoculated (0.1% each) into 50 mL of BG11-Pt or BG11-Pi media. The cultures were incubated at 30 °C with bubbling for 15 days and spread onto BG11-Pt agar medium for detecting viable RH714 cells or onto BG11-Pi agar medium to detect wild-type strains.

## 2.3 Results and Discussion

### 2.3.1 Replacement of HtxB signal peptide for functional expression of the Htx transporter in *Syn* 7942

The HtxBCDE transporter of *P. stutzeri* WM88 which selectively takes up Pt but not Pi, is an important element of the Pt-dependent biocontainment strategy (Figure 2.1) (27).

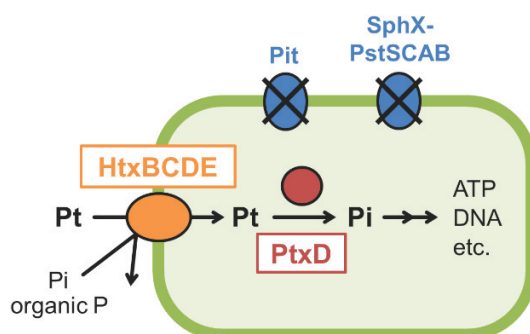


**Figure 2.1** Simplified schematic representing the P metabolic pathway engineered for the containment of *Syn* 7942. Construction of the Pt-dependent strain was achieved by disrupting the endogenous phosphate (Pi) transporters and exogenously expressing HtxBCDE and PtxD. HtxBCDE expression enables the uptake of phosphite (Pt) but not Pi or organic P compounds. The incorporated Pt is oxidized by PtxD to Pi, the metabolically available form for assimilation.

I first examined whether HtxBCDE might be expressed functionally in *Syn* 7942. Since *Syn* 7942 lack Pt oxidizing activity, I combined the *ptxD* gene of *Ralstonia* sp. 4506 (5) to the *htxBCDE* operon and integrated the fused DNA into the neutral site 1 (NS1) of the genome (Figure 2.2A). However, the resultant strain RH683 exhibited nearly no growth in the BG11 medium containing Pt as the sole P source (BG11-Pt) (Figure 2.2B). Cyanobacterial cells, unlike many

other bacteria, are distinctly compartmentalized by complex membrane structures made up of thylakoids and plasma membranes (33). Therefore, i expected that improper localization of the wild-type HtxBCDE is the reason for non-functional expression in *Syn 7942*. Despite the fact that the protein sorting mechanisms in *Syn 7942* are not fully known, numerous studies have indicated the role of signal peptide (SP) sequences at the N-termini of target proteins in the proper localization of proteins across and into membranes (33, 34). HtxBCDE is a member of the ATP-binding cassette (ABC) transporter family that facilitates solute uptake and generally consists of a periplasmic substrate-binding protein with a unique SP sequence (35). As anticipated, predictive analysis showed a putative SP sequence in the substrate-binding protein HtxB (Figure 2.2A). To evaluate the compatibility of the SP sequence with *Syn 7942*, i swapped the wild-type SP of HtxB with three different SPs from other periplasmic proteins (the PtxBs from *Anabaena* sp. PCC 7120 (30) [hereafter *Ana 7120*] and *Ralstonia* sp. 4506 (27), and PstS from *Syn 7942* (31)) (Figure 2.2A). On BG11-Pt medium, only the cells of strain RH693, which contained the modified HtxB with the SP from the PtxB protein of *Ana 7120*, grew well compared to the other strains (Figure 2.2B). By using an anti-HtxB antibody, immunoblot analysis demonstrated that both the RH683 and RH693 strains expressed HtxB protein ( Figure 2.3). As a result, the failure of RH683 to grow on Pt is most likely due to the inappropriate localization of the HtxB protein. Overall, our findings demonstrated that the SP of *Ana 7120* PtxB is consistent with the functional expression of HtxB in *Syn 7942*.

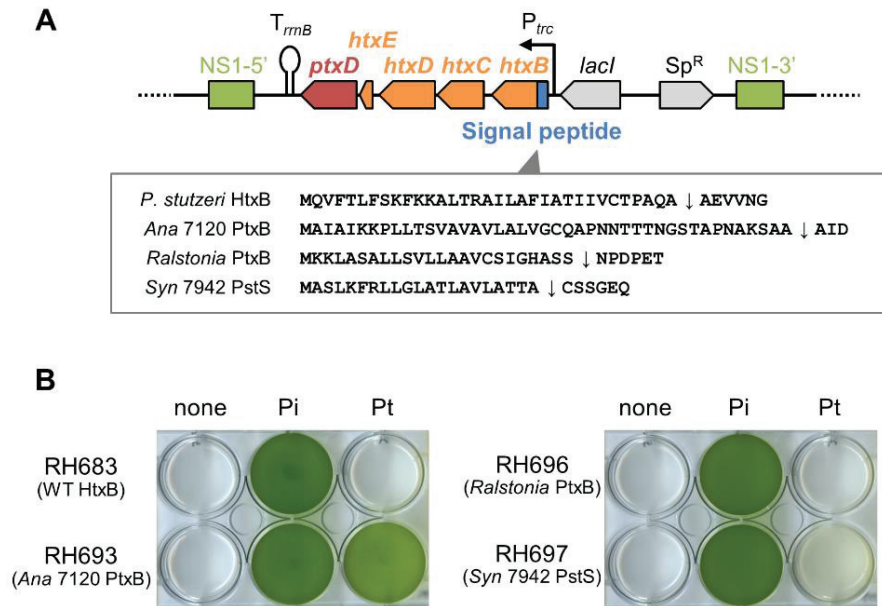


**Figure 2.2** Compatibility of different signal peptide (SP) sequences for the functional expression of the Htx transporter in *Syn* 7942. (A) Schematic representing the structure of the expression cassette for HtxBCDE and PtxD, integrated into the neutral site 1 (NS1) of the *Syn* 7942 genome. The *htxBCDE* operon is transcriptionally fused to *ptxD* and is under the control of the IPTG inducible promoter  $P_{trc}$ . The SP sequence of HtxB was replaced with that of *Ana* 7120 PtxB, *Ralstonia* PtxB, or *Syn* 7942 PstS. Down arrows in the SP sequences indicate the cleavage sites predicted with the Sigcleave tool of EMBOSS (59).  $Sp^R$ , spectinomycin resistance gene;  $T_{rrnB}$ , transcriptional terminator. (B) Growth of *Syn* 7942 strains containing the expression cassettes in BG11 media. Cells grown on BG11-Pi agar plates were inoculated and cultured in BG11 media containing 0.2 mM Pi, Pt, or no source of P. The photographs were taken after 7 days of incubation. The data are representative of three biological replicates with essentially the same results.

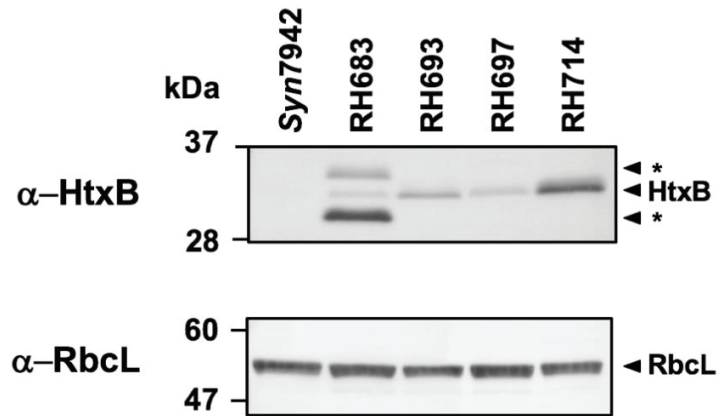


**Figure 2.3** Immunoblot analysis of proteins from *Syn 7942* expressing HtxB with different signal peptide sequences. Total cell extracts from the wild-type strain (*Syn7942*), RH683, RH697, and RH714 were separated by SDS-PAGE and the gels were subjected to immunoblot analysis. RbcL was used as a loading control. It should be noted that the difference in the molecular weights of the bands detected by anti-HtxB antibody in RH683 is probably due to the different processing of the signal peptide of the HtxB protein in *Syn 7942* (marked by stars “\*”).

### 2.3.2 Identification of endogenous Pi transporters in *Syn 7942*

The deletion of endogenous transporters involved in P uptake from various sources is another necessity for the containment strategy (Figure 2.1). *In silico* analysis revealed that *Syn 7942* contains two types of Pi transporter, Pit and Pst, but no transporters for organic P compounds such as Pi esters and phosphonates (Pn). PstSCAB of *Syn 7942* is an ABC-type Pi transporter with an extra substrate-binding protein, SphX, besides PstS (31). There is no direct evidence that the homologue of Pit mediates Pi transport, although the Pi uptake kinetics of *Syn 7942* clearly suggest the presence of numerous uptake systems with different kinetic properties (36). Therefore, I characterized the Pit homologue using *E. coli* MT2012-*ptxD* (27), a strain lacking all endogenous Pi transporters (PitA, PitB, PstSCAB, and PhnCDE) but containing *ptxD* gene from *Ralstonia*, as a host strain to assess both the Pi and Pt transport activities of *Syn 7942* Pit. I transformed the *pit* homologue from *Syn 7942* (Synpcc7942\_0184) into MT2012-*ptxD* and cultivated the transformants on morpholinopropane sulfonic acid (MOPS)-minimal medium containing Pi (MOPS-Pi) or Pt (MOPS-Pt) as the sole P source. I found the transformants carrying Synpcc7942\_0184 were able to grow on MOPS-Pi similar to strain carrying *E. coli* PitA used as a positive control. These findings indicated that the *Syn 7942 pit* homologue encodes a functioning Pi transporter and is a target gene that requires to be disrupted in order to create Pt-dependent strains.

### 2.3.3 Pt-dependent *Syn 7942* strain construction

I proceeded to create a Pit and Pst double mutant of strain RH693 that express PtxD and HtxBCDE with the modified SP of HtxB of *Ana 7120*. Gene disruption was sequentially carried out by allelic replacement, initially for the *pit* gene (Synpcc7942\_0184) (Figure 2.4A) and subsequently for the *sphX-pstSCAB* operon (Synpcc7942\_2441 to 2445) (Figure 2.4B). The

generating disruptant was screened on BG11-Pt or -Pi media. The double mutant strains RH714, RH715, and RH716 were only completely segregated when screened on BG11-Pt agar plates (Figure 2.4B), but not on BG11-Pi agar plates. Furthermore, the double mutants failed to grow on BG11-Pi agar plates, although the wild-type and PtxD/HtxBCDE-expressing strain (RH693) strain could (Figure 2.5A). These findings clearly suggested that *Syn 7942* includes no additional Pi transporters except Pit and Pst, and, therefore, Htx is the only transporter that facilitates P uptake in the double mutant. In liquid culture experiments, the double mutants were unable to grow in BG11-Pi media (Figure 2.5B). The same growth profiles have been found of different clones of the double mutant strains RH714, RH715, and RH716, indicating that the Pt dependency is a stable phenotype. The mutants' final optical densities in BG11-Pt medium were in the range 6.5–7.5, which is nearly 30% lower than that of the wild-type strain grown on BG11-Pi medium. I measured the concentration of P source in the culture supernatant of wild type and RH714, to know the reason for the reduced growth of the Pt-dependent strains. I observed that both strains consumed complete P sources during their growth (Figure 2.6). As a result, differences in the growth between the strains cannot be explained by the amount of P consumed by the cells. However, the Pt concentration in the RH714 culture decreased more slowly than the Pi concentration in the wild-type culture. Pi is necessary as a primary substrate for DNA synthesis, and DNA replication activity in *Syn 7942* is higher in early growth phases than in late exponential and linear phases. Therefore, insufficient P source availability in the early growth phase may have an impact on RH714 subsequent growth. Bisson et al. recently reported that the Pt affinity of HtxB was very low ( $K_d > 10$  mM) (30). As a result, this growth retardation could be restored by enhancing the Pt affinity of HtxB protein. PtxD also oxidizes Pt to Pi coupled with the reduction of  $\text{NAD}^+$  to NADH (3). Although no direct evidence has been obtained, Pt assimilation may imbalance the intracellular

NADH/NAD<sup>+</sup> ratio of RH714, which can affect cellular physiology. Previously, the growth rate of the Pt-dependent *E. coli* strain on Pt medium was 93% of that of the wild type cultured on Pi (27). Thus, maintaining the optimization of the intracellular phosphorus flux or redox balance will improve the growth rate of Pt-dependent cyanobacteria.

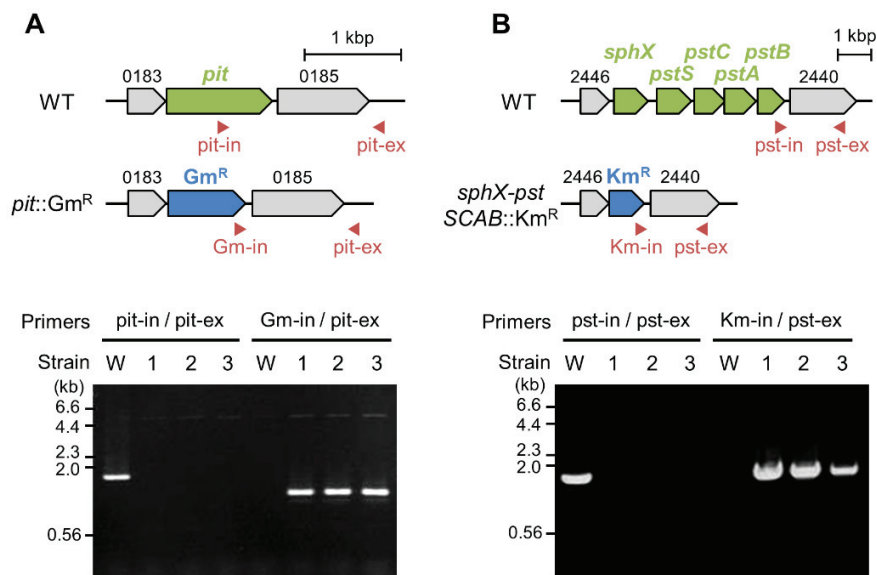


**Figure 2.4** Disruption of endogenous Pi transporter genes in *Syn 7942*. Schematic diagrams (top) represent the genomic organization around the (A) *pit* and (B) *sphX-pstSCAB* genes. Deletion mutants of the genes were generated by homologous recombination that replaced the *pit* and *sphX-pstSCAB* genes with Gm<sup>R</sup> and Km<sup>R</sup> cassettes, respectively. Complete segregation of the mutants was confirmed by PCR (bottom) using the appropriate primer pairs indicated by arrowheads in the upper panel. The target sizes of each PCR product were 1.63 kb for pit-in/pit-ex, 1.18 kb for Gm-in/pit-ex, 1.64 kb for pst-in/pst-ex, and 1.65 kb for Km-in/pst-ex. W: wild-type; 1: strain RH714; 2: RH715; 3: RH716.

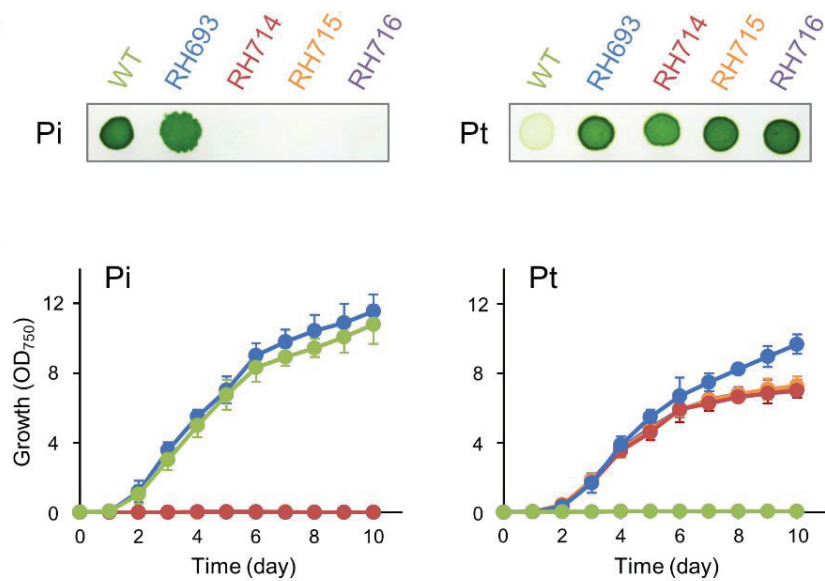


**Figure 2.5** Growth of RH714 and related strains on BG11 media. (A) Growth on agar plates. Cells were spotted onto BG11-Pi or BG11-Pt agar plates and incubated for 14 days. The wild-type strain appeared to grow slightly on BG11-Pt agar, probably owing to the presence of intracellular P storage that can be used as P sources. (B) Growth curve in liquid media. The wild-type (green), RH693 (blue), RH714 (red), RH715 (orange), and RH716 (purple) strains were cultured in BG11-Pi or BG11-Pt liquid media. Cell growth was monitored every day by measuring turbidity at 750 nm. The error bars represent the standard deviation of three biological replicates.

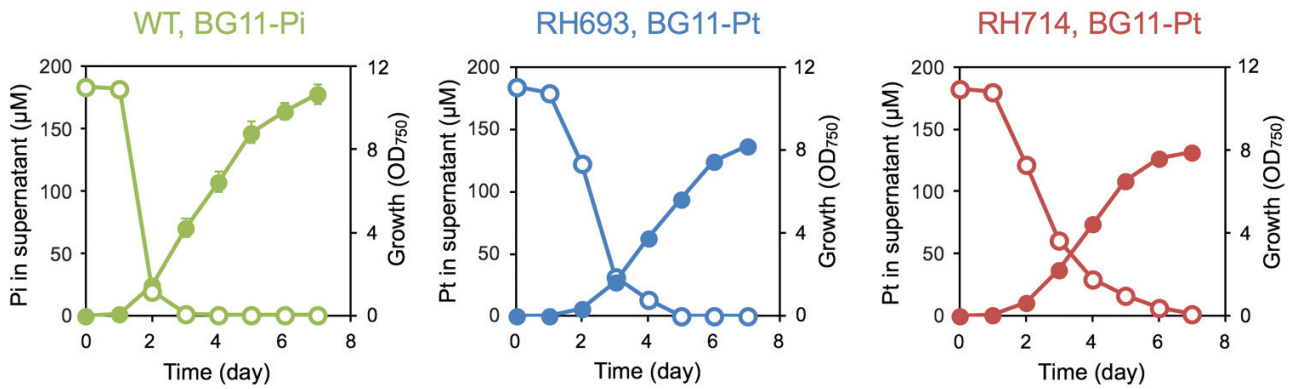


**Figure 2.6.** Growth and P source assimilation of *Syn* 7942 wild-type, RH693, and RH714. The wild-type was cultured in BG11-Pi, and the strain RH693 and RH714 were grown on BG11-Pt media. Cell growth (filled circles) was monitored every day by measuring turbidity at 750 nm. Pi and Pt concentrations in the culture supernatants (open circles) were determined by malachite green method and ion chromatography, respectively. The error bars represent the standard deviation of three biological replicates.

#### 2.3.4 Availability of P sources for strain RH714

To evaluate the growth of RH714 strain on other P sources, the cells were cultured in BG11 media containing several types of P compounds found in the natural environment. Because inorganic phosphorus, including Pi, is found in limited amounts in many aquatic environments, dissolved organic phosphorus (DOP) is recognized as the main P source in the hydrosphere (37,38). Phosphoesters, a large portion of the DOP in ecosystems (39), are easily accessible sources of P because they may be hydrolyzed by extracellular and periplasmic phosphatases to release Pi, which can then be taken up by transporters such as Pit and Pst (40). Indeed, by utilizing two different types of alkaline phosphatases, namely PhoA and PhoV, the wild-type *Syn* 7942 strain may grow on BG11 medium containing glucose 6-phosphate (G6P) (Figure 2.6) (41,42). The phosphatases of *Syn* 7942, like many other alkaline phosphatases, function by cleaving the phosphoanhydride bond between inorganic pyrophosphate (PPi) and Pi moieties within ATP, releasing Pi that acts as a P source (Figure 2.7). Despite the presence of both phosphatases, RH714 is unable to grow on these P sources (Figure 2.7). Moreover, DNA serves as a P source for *Syn* 7942 after digestion by the putative nuclease Synpcc7942\_1000 (43) and following hydrolysis by alkaline phosphatases (Figure 2.7). However, RH714 failed to grow on DNA supplemented medium (Figure 2.7). Phosphonates, which are organic P compounds with a covalent carbon–phosphorus (C–P) bond, are measurable components of DOP in some freshwater habitats (44,45). Several studies have found that the genes implicated in phosphonate uptake and metabolization are widely distributed in environments where freshwater cyanobacteria grows (46,47). However, aminoethylphosphonate and methylphosphonate, two types of phosphonates, cannot support the growth of wild-type *Syn* 7942 or strain RH714 (Figure 2.7), possibly due to the lack of phosphonate uptake and/or assimilation genes. I conducted growth assays using BG11 media made with

sterilized pond or river water to assess the effect of the presence of P sources in freshwater ecosystems. RH714 failed to grow on these media even when  $P_i$  was externally added (Figure 2.7), suggesting that the freshwater P sources cannot support the growth of strain RH714. Taken together, these findings clearly suggest that RH714 cannot grow in natural environments.

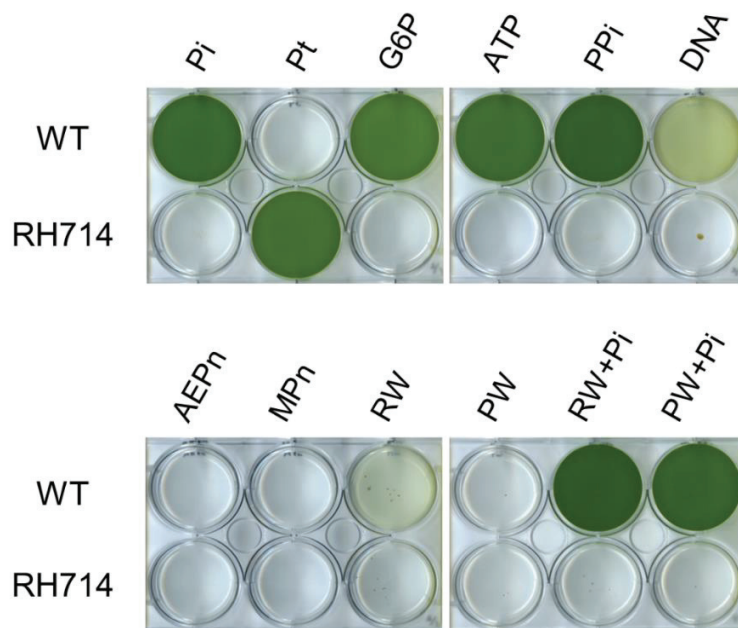


**Figure 2.7** Growth of RH714 in BG11 media containing different P sources. Commercially available P sources (Pi, Pt, glucose 6-phosphate [G6P], ATP, pyrophosphate [PPI], DNA, aminoethylphosphonate [AEPn], and methylphosphonate [MPn]) were added at concentrations equivalent to 0.2 mM Pi. BG11-RW (RW) and BG11-PW (PW) were prepared using pond water and river water, respectively. They were supplemented with 0.2 mM Pi to prepare RW+Pi and PW+Pi, respectively. The photographs were taken after incubation for 7 days. The data are representative of two biological replicates with essentially the same results.

### 2.3.5 Escape frequency and long-term viability

Next, the author evaluated the development of escape mutants under Pi conditions in order to confirm the efficacy of the Pt-dependent containment approach for cyanobacteria. On BG11-Pi agar plates, approximately  $2.8 \times 10^{10}$  RH714 cells were spread and cultured for 28 days. No colonies have been observed, indicating that RH714 does not yield escape mutants with an assay detection limit of  $3.6 \times 10^{-11}$  per colony forming unit (CFU). This frequency is comparable to other cyanobacteria containment strategies (48), and it is at least three orders of magnitude lower than the limit recommended by the NIH ( $10^{-8}$  per CFU) (49).

To investigate the survival rate of RH714, approximately  $10^{10}$  cells were cultured in both BG11-Pt and -Pi media before being plated onto BG11-Pt agar to determine viable cells. The viability of RH714 steadily declined during cultivation in the Pi-based medium, and dropped below the detection limit within 14 days of inoculation (Figure 2.8A). Surprisingly, after 12 days, the cells clearly seemed to undergo chlorosis (Figure 2.8B), which is known to be caused by nutrient depletion (50). Over 14 days of cultivation in the BG11-Pt medium, on the other hand, the cells observed no decrease in the number of CFU and no differences in appearance (Figures 2.8A, B). These findings demonstrate that the survival rate of RH714 rapidly decreases in the absence of Pt. The generation of escape mutants that persist in the aquatic habitat is considered the worst-case scenario in the release of engineered algae. The contained strain generated in this study with limited viability in the absence of Pt significantly reduces the possibility of such an undesirable outcome.

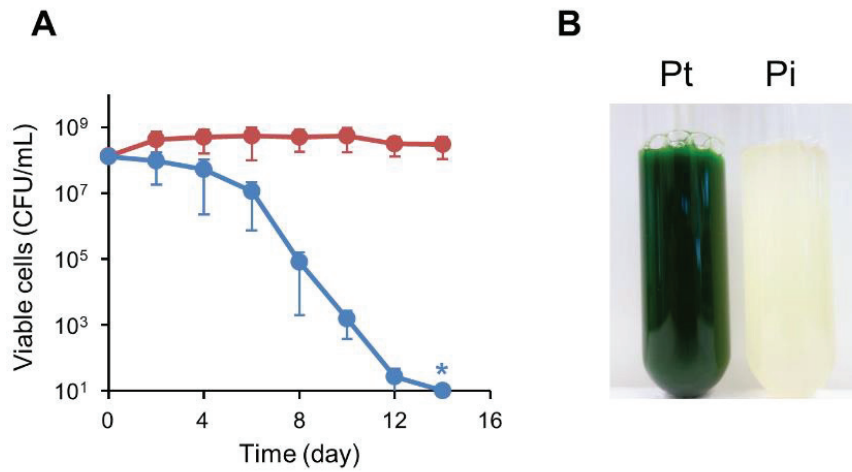


**Figure 2.8** Long-term viability of strain RH714. (A) Viability of cells in BG11 media over time. Approximately  $10^{10}$  RH714 cells cultured in BG11-Pt medium were incubated in either BG11-Pt (red) or BG11-Pi (blue) media. The viable cells were counted by plating on BG11-Pt agar medium. Asterisks indicate no colonies were detected. The error bars represent the standard deviation of four biological replicates. (B) Image of the cultures in BG11-Pt (Pt) or BG11-Pi (Pi) media taken 14 days after inoculation.

### **2.3.6 Growth competition between RH714 and wild-type cyanobacteria**

To assess the ability of RH714 strain to outcompete contaminating microbes in media containing Pt as the sole P source, RH714 cells were co-cultured with wild-type *Syn* 7942 and *Synechocystis* sp. PCC 6803 (hereafter *Syn* 6803) in BG11-Pt and -Pi liquid media. Each wild-type strain was simultaneously inoculated with approximately 10-times the number of RH714. After 15 days of cultivation, RH714 dominated the Pt-based medium, accounting for >97% of the total cells (Table 2.4). On the other hand, the wild-type strains dominated the population when cultivated in BG11-Pi medium (Table 2.4). Then, I carried out direct PCR on the colonies growing on BG11-Pt from a co-culture of RH714 and *Syn* 6803 to verify that the growing cells on BG11-Pt medium in a co-culture experiment were indeed RH714. I found that all checked colonies were RH714, demonstrating that no horizontal gene transfer effects were observed under the co-culture conditions (Figure 2.9). Overall, these findings indicate that RH714 has a competitive growth advantage in a Pt-based medium over possible contaminants, allowing for selective growth in the presence of other microalgae.

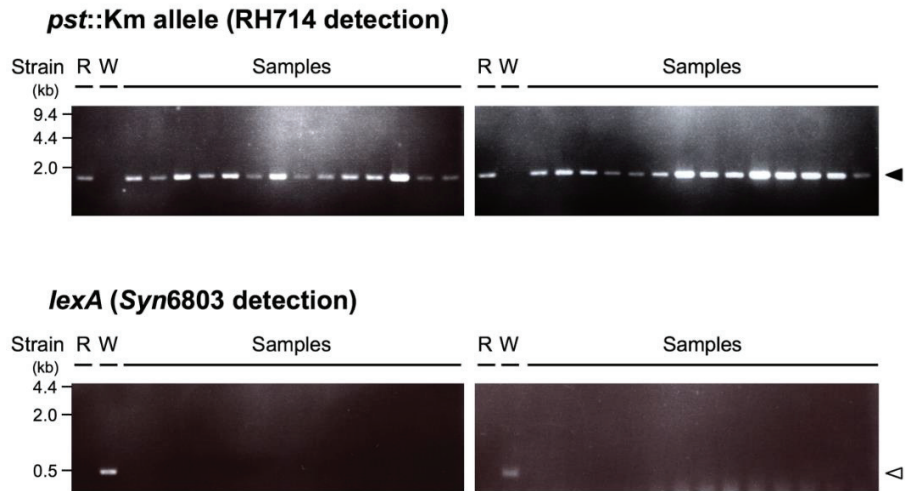


**Figure 2.9** Confirmation of the strains growing in mixed culture on Pt-based media. Strains of randomly selected colonies were determined by allele-specific PCR to detect *pst::Km* allele in RH714 and *lexA* in *Syn 6803*, respectively. Pictures are representative of 28 samples. The target sizes of each PCR product were 1.65 kb for Km-in/*pst*-ex (black arrowhead) and 0.53 kb for *lexA*-F/*lexA*-R (white arrowhead). R: RH714; W: *Syn 6803* wild type.

In this part of my study, I established that engineered Pt-dependency is a viable strategy for biological containment of cyanobacteria. My findings suggest that this strategy can be used for a wide range of other microorganisms due to its simplicity. In contrast to the chemicals necessary for other biocontainment strategies, Pt is inexpensive, allowing us to operate economically feasible microalgal cultivation on a large scale. One concern associated with our strategy is that the Pt-dependent strain might acquire Pi transport genes through horizontal gene transfer. Because the modelled cyanobacteria, involving *Syn 7942*, have a high natural competence (51), transferring foreign DNA carrying Pi transporter genes could restore the cells' ability to uptake Pi, allowing them to escape from the containment. To decrease such concerns, disruption of genes associated with natural competence would be an efficient approach. In several bacteria species, ComEC, a cytoplasmic membrane channel for DNA uptake, is critical for natural competence (52,53). It has been noted that the deletion of the *comEC* genes in *Synechococcus* sp. PCC 7002 results in the loss of natural competence (48). The *hfq* gene in cyanobacteria encodes an RNA chaperone that binds to the base of the Type IV pilus, and disruption of *Syn 6803* and *Synechococcus* sp. PCC 7002 equivalents eliminates their natural competency (48,54). *Syn 7942* contains the competence-related genes *comEC* (*Synpcc7942\_2458*) and *hfq* (*Synpcc7942\_1926*). As a result, disrupting these genes may alleviate the risks of engineered strains escaping containment through horizontal gene transfer. The risk of horizontal gene transfer may also be decreased by implementing redundant containment strategies that are based on different principles. As previously stated, our strategy can be easily merged with variant containment methods due to the simplicity of the genetic modifications.

In contrast to other biocontainment strategies previously reported, the modified Pt-dependent cells established in our study exhibited a competitive growth advantage over most

contaminants (which cannot assimilate Pt). In a mixed culture supplemented with Pt, Loera-Quezada and colleagues revealed that the introduction of the *ptxD* gene of *P. stutzeri* allowed the microalga *Chlamydomonas reinhardtii* to become as the dominant species (25) the author also showed that Pt-dependent cyanobacteria could simply dominate in BG11-Pt medium (Table 2.4). This advantage can significantly improve productivity and decrease the risks of the development of escape mutants that acquire Pi-transporter genes from contaminants, which is a unique feature of our biocontainment strategy. One drawback of contamination risk management in this strategy is its incompatibility with the use of Pi-containing wastewater as a water source. Recently, several

**Table 2. 4** Growth competition between RH714 and wild-type cyanobacteria <sup>a</sup>

P source	Wild-type strains / RH714 ratio	
	day 0	day 15
Pi	18 ( $2.1 \times 10^4$ cells)	$3.8 \times 10^6$ ( $5.7 \times 10^8$ cells)
Pt	24 ( $2.5 \times 10^4$ cells)	$2.9 \times 10^{-2}$ ( $6.3 \times 10^8$ cells)

<sup>a</sup>The numbers in parentheses are the total cell numbers of cyanobacterial strains.

studies have suggested incorporating cultivation of microalgae for wastewater treatment as a cost-effective strategy for biofuel production (55). However, such water sources could reduce the selectivity of Pt-dependent strains due to introducing Pi into culture media, allowing contaminants to grow. Thus, to limit Pi input and ensure the effect of culture selectivity when Pi-containing wastewater is used, a treatment such as enhanced biological phosphate removal is required (56).

## **Chapter 3**

### **Engineering cofactor specificity of RsPtxD toward NADP**

### 3.1 Introduction

In this chapter, the author has engineered the cofactor specificity of RsPtxD that might be useful for *in vitro* applications. Biocatalysts have been extensively used in the chemical, pharmaceutical, and energy industries (60-62). The number of enzymes utilized as catalysts in various biotechnology-related fields has increased dramatically over the last few years and is continuing to grow (63,64). Their catalytic efficiency under benign reactions paired with high selectivity makes them valuable tools for sustainable industrial processing (62,65,66). Furthermore, recent progress in genomics, metagenomics, and synthetic biology expanded substantially the number of enzymes available for use as a particular biocatalyst in bioproduction. However, the majority of industrially used enzymes (over 65%) only catalyze simple cofactor-independent reactions, and more complicated enzymatic reactions are still unused due to their requirement for one or more costly cofactors (67,68). Dehydrogenases, in particular, need nicotinamide cofactors, NAD(H) or NADP(H), to catalyze a variety of industrially useful reactions such as chiral conversions of pharmaceutical building blocks, which prevents their addition in stoichiometric amounts for large-scale synthesis (69,70).

The ideal solution to these limitations, is *in situ* cofactor regeneration by recycling catalytic pools of cofactors using inexpensive available sacrificial substrates (71). Due to the thermodynamically strong driving force of the regeneration reaction, implementation of such cofactor regeneration system can decrease production costs and enhanced productivity by obviating product inhibition and/or by promoting the main reaction (72,73). The methods for cofactor regeneration are generally classified into four categories: chemical, photochemical, electrochemical, and enzymatic reactions (72). However, for wider utilization, the enzymatic

approach is a very promising strategy based on exquisite selectivity, compatibility with enzyme catalyzed synthesis, and high efficiency compared to other methods (67).

Currently, there are numerous enzymes for NADH cofactor regeneration system that have been known, including formate dehydrogenase (FDH) (71), alcohol dehydrogenase, glucose 6-phosphate dehydrogenase, and glucose dehydrogenase (GDH), (74,75). The most extensively utilized enzyme is FDH from *Candida boidinii*, which has been exhibited to support the production of *L-tert*-leucine on a multi-ton scale (76). GDH and FDH are further utilized as an NADPH regeneration system. Due to its higher specific activity and an inexpensive substrate (glucose), GDH is superior. Meanwhile, FDH provides a strongly driven reaction because of its free-energy changes, and the reaction's by-product, CO<sub>2</sub>, does not affect the reaction's conditions. Although FDHs naturally isolated from bacteria are unable to accept NADP as a cofactor, NADP-dependent FDH mutant from *Pseudomonas* sp. 101 (mut-PseFDH) was developed, and it was utilized to regenerate NADPH for chiral (*R*)-alcohols and lactones production (77,78). Both GDH and FDH, however, have disadvantages; GDH generates gluconic acid as a by-product, which inhibits the main reactions due to pH fluctuations during reactions (76). The catalytic efficiency of FDH is lower than other regeneration enzymes (79). As a result of the high cost of NADPH and the lack of a good regeneration system, many valuable of NADPH-dependent enzymes are idle. Therefore, developing a highly active and economically feasible NADPH regenerative enzyme for bioindustrial manufacturing is crucial.

Phosphite dehydrogenase (PtxD), which catalyzes the nearly irreversible oxidation of phosphite to phosphate coupling with the reduction of NAD, was initially isolated from *Pseudomonas stutzeri* WM88 (PsePtxD) (3). Following this discovery, PtxD have been isolated from a variety of bacteria found in inhabits including soils and aquatic environments (5,21). Owing

to many practical advantages, PtxD has received substantial research attention as an alternative cofactor regeneration system: first, higher NADH regeneration by PtxD than any other NADH regeneration enzyme due to the large change in free energy of this reaction ( $\Delta G^\circ = -63.3$  kJ/mol); second, phosphate produced as a by-product by Pt oxidation can act as a buffer for the main reaction (80,81); and third, phosphite is also available from the by-products of numerous industrial processes, thus ensuring an economically feasible reaction process (4). Since heterologous expression of PtxD can expand the phosphorus substrate repertoire of various organisms, PtxD has also received an increased attention as a tool for selective cultivation (23,26) and biological containment of bacteria (27, 82). However, originally isolated PtxD enzymes, including PsePtxD, generally exhibit low thermostability and accept NADP as a substrate very poor, which limited their utilization as a practical NADPH regeneration system. As a result, Johannes and colleagues engineered a PsePtxD generating a thermostable mutant (12 $\times$ ) with approximately 7,000-fold higher half-life at 45°C of heat inactivation than that of the wild-type enzyme (83). Meanwhile, Woodyer et al. successfully relaxed its cofactor specificity by creating a double mutant PsePtxD (PsePtxD<sub>E175A/A176R</sub>) with two amino acid residues substitutions at the NAD-binding site in the Rossmann-fold domain (84). However, the introduction of these two mutations into 12 $\times$  mutant simultaneously was not consistent, and the NADPH regeneration reaction of the derivative variant (12 $\times$ -A176R) exhibited catalytic efficiency of around 15 $\mu\text{mol}^{-1} \text{min}^{-1}$  and evaluated only at a lower temperature ( $\sim 25^\circ\text{C}$ ) (85).

One of the important features for industrial biocatalyst is thermostability due to its ability to robust and expand the operating temperature range. Previously, Hirota et al., isolated PtxD from a soil bacterium *Ralstonia* sp. 4506 (RsPtxD), which exhibited a 3,450-fold longer half-life at 45°C (80.5 h) than that of PsePtxD. The catalytic efficiency of RsPtxD was 7-times higher than PsePtxD

and has a 54% amino acid sequence similarity to PsePtxD (5). However, the capability of RsPtxD to utilize NADP is very poor (5), hindering the use of the enzyme as an NADPH regeneration system.

In this part of our study, i evolved RsPtxD mutants with improved specificity toward NADP and higher thermostability. The biochemical analysis revealed that the NADP binding affinity of RsPtxD mutants was drastically improved, which contributed to not only increased heat stability, but also increased tolerance to organic solvents. The ability of RsPtxD mutant to utilize it as an NADPH regeneration system was assessed during the conversion of 3-dehydroshikimate (3-DHS) to shikimic acid (SA) at 45°C by a thermophilic shikimate dehydrogenase from *T. thermophilus* HB8.

## **3.2 Experimental Section**

### **3.2.1 RsPtxD mutant's creation using site-directed mutagenesis**

The expression plasmids of the His-tagged RsPtxD mutants were created with specific primer pairs from *RsptxD/pET21b* plasmid (5) using a PrimeSTAR Mutagenesis Basal Kit (TaKaRa Bio, Shiga, Japan) (Table 3.1). The PCR reaction was carried out according to the manufacturer's instructions, and all mutant genes were sequenced to confirm the desired mutation.

**Table 3.1** The oligonucleotides and plasmids used in this study

Primers	Sequence 5'-3'*
D175A/P176R_fw	TTG <b>CGCACGT</b> ATTCCGCTCAATGCCGAA
D175A/P176R_rv	GGAAT <b>ACGTGCG</b> CAATACCAGAGATTCA
C174H/D175A/P176R_fw	TGTAT <b>CACGCACGT</b> ATTCCGCTCAATG
C174H/D175A/P176R_rv	ACGT <b>GCGTG</b> AACAAGAGATTCATTTC
C174H/D175A/P176R/ I177K/P178A_fw	GCACGT <b>AAAGCG</b> CTCAATGCCGAACAAG
C174H/D175A/P176R/ I177K/P178A_rv	TGAG <b>CGCTTT</b> ACGTGCGTGATAACAAGAG
C174H/D175A/P176R/ I177R/P178A_fw	GCACGT <b>CGCGCG</b> CTCAATGCCGAACAAG
C174H/D175A/P176R/ I177R/P178A_rv	TGAG <b>CGCGCG</b> ACGTGCGTGATAACAAGAG
Plasmids	Descriptions
<i>RsptxD</i> /pET21b	pET21b (Novagen) containing <i>RsptxD</i> (5)
<i>RsptxD</i> <sub>(D175A/P176R)</sub> /pET21b	pET21b containing a mutant <i>RsptxD</i> gene for RsPtxD <sub>AR</sub> expression
<i>RsptxD</i> <sub>(C174H/D175A/P176R)</sub> /pET21b	pET21b containing a mutant <i>RsptxD</i> gene for RsPtxD <sub>HAR</sub> expression
<i>RsptxD</i> <sub>(C174H/D175A/P176R/I177K/P178A)</sub> /pET21b	pET21b containing a mutant <i>RsptxD</i> gene for RsPtxD <sub>HARKA</sub> expression
<i>RsptxD</i> <sub>(C174H/D175A/P176R/I177R/P178A)</sub> /pET21b	pET21b containing a mutant <i>RsptxD</i> gene for RsPtxD <sub>HARRA</sub> expression
<i>sdh</i> /pET11a	pET11a plasmid containing shikimate dehydrogenase gene from <i>T. thermophilus</i> (87)

\*Boldface nucleotide sequences indicate mutation positions.

### 3.2.2 Overexpression and purification of RsPtxD proteins

For the expression of mutant RsPtxD proteins, the *RsptxD* mutant plasmids were transformed into *Escherichia. coli* Rosetta 2 (DE3) pLysS (Novagen) and grown overnight at 37°C in the 2×YT liquid medium (86). The cells were inoculated in 50 mL of fresh medium and cultured at 37°C until they reached an optical density at 600 nm (OD<sub>600</sub>) of around 0.5. Then, 0.2 mM of isopropyl β-D-thiogalactopyranoside (IPTG) was added to induce protein expression at 28°C for 6 hours. The cells were harvested by centrifugation and resuspended in 5 mL of 20 mM Tris–HCl (pH 7.4), 50 mM NaCl, and 20% glycerol. The cell pellets were lysed using sonication on ice for 4 min with a pulse sequence of 1 s on and 2 s off at 20% amplitude level. To remove the cell debris, the crude extracts were then centrifuged at 20,000 ×g for 30 min at 4°C. The Histidine-tagged recombinant proteins in the supernatant were filtered through a 0.45-μm filter and loaded onto a 1 mL HisTrap HP column (GE Healthcare UK Ltd., Little Chalfont, UK) equilibrated in buffer A [20 mM Tris–HCl (pH 7.4), 50 mM NaCl, and 20% glycerol]. the column was washed with 10 mL of buffer A after proteins were bound, and eluted with a linear 10 mL gradient of 0–0.5 M imidazole in buffer A. The eluted protein fractions were pooled, and the buffer was replaced to 50 mM Tris–HCl (pH 7.4) and 15% glycerol by ultrafiltration using Amicon Ultra centrifugal filtration devices (10 kDa molecular mass cutoff) (Merck Millipore, Darmstadt, Germany).

For the expression of shikimate dehydrogenase (SDH), *E. coli* Rosetta 2 (DE3) pLysS was transformed with plasmid pET-11 harboring a gene encoding SDH from *T. thermophilus* HB8 genome (87). The protein expression was induced in the same way as stated above , with the exception that IPTG concentration in the culture was 0.4 mM. The cells were harvested and suspended in 20 mM Tris–HCl (pH 8.0) containing 50 mM NaCl and 20% glycerol, disrupted as described above before being heated at 80 °C for 10 min to inactivate the *E. coli* proteins. After

that, the cell debris and denatured proteins were removed by centrifugation at 20,000  $\times g$  for 30 min. The filtered crude extract was applied onto a 5 mL HiTrap SP FF column (GE Healthcare UK Ltd., Little Chalfont, UK) equilibrated with a buffer containing 50 mM HEPES (pH7.0) and 15% glycerol. In the same buffer, The SDH protein was eluted with a linear gradient of 0–1.0 M NaCl. The fractions containing SDH were collected, and the solution was substituted as described above.

### 3.2.3 Enzyme kinetics analysis

The experiments were carried out in solutions containing phosphite, NAD(P), 5  $\mu\text{g}/\text{mL}$  PtxD protein, and 100 mM morpholinepropanesulfonic acid (MOPS, pH 7.3). For determined kinetic constants for one substrate at least five varying concentration was used, while the other substrate was added at saturated concentrations (1 mM). Initial rates were carried out by monitoring the increase in absorbance NAD(P)H ( $6,220 \text{ M}^{-1} \text{ cm}^{-1}$ ) at 340 nm, using a Beckman DU-800 spectrophotometer (Beckman Coulter, CA, USA). The kinetic constants,  $K_M$  and  $k_{\text{cat}}$ , for NAD(P) and phosphate were given using the Lineweaver–Burk plots. .

### 3.2.4 Optimal temperature for RsPtxD proteins

The optimal temperature assays were determined by incubating the reaction mixture at varying temperatures. The activities of the RsPtxD mutants were measured in 20 mM MOPS (pH 7.3) in the presence of 0.5 mM NAD(P) and 2.0  $\mu\text{g}/\text{mL}$  of RsPtxD proteins in a reaction volume of 0.5 mL. The reaction was initiated after adding phosphite at a final concentration of 1 mM into the mixture, and NAD(P)H production was monitored at absorbance 340 nm for 30 min. The enzyme activity was defined as a relative activity of the residual activity relative to maximum activity and each assay repeated three times.

### 3.2.5 Thermostability and organic solvents tolerance of RsPtxD variants

The thermostability assay was carried out according to Woodyer et al. (84) with minor modifications. To assess the effects of NAD(P) binding with RsPtxD mutants on thermostability, a 0.2 mL solution containing 0.2  $\mu\text{g}/\mu\text{L}$  of the RsPtxD mutant in 50 mM MOPS (pH 7.3) was preincubated on ice with or without 0.5 mM NAD(P) for 5 min and incubated at 45°C. A 10  $\mu\text{L}$  aliquot was taken at different times, and the residual activity was measured in the solution containing 0.5 mM NAD(P), 1.0 mM phosphite, and 20 mM MOPS (pH 7.3) at 37°C in a 1.0 mL reaction volume. To investigate the organic solvent tolerance of RsPtxD mutants, a 0.2 mL solution containing 0.2  $\mu\text{g}/\mu\text{L}$  of the RsPtxD mutant in 50 mM MOPS (pH 7.3) was preincubated with or without NAD(P) for 5 min then incubated with different concentrations of *N,N*-dimethylformamide (DMF) at room temperature (25°C) for 6 h. The residual PtxD activity was assayed as described above.

### 3.2.6 Optimal pH for RsPtxD proteins

The activity of the RsPtxD mutants in the pH range of 6.2–9.2 was determined using buffers 2-morpholinoethanesulfonic acid (MES, pH 6.2), MOPS (pH 7.3), Tris (pH 8.0), and *N*-cyclohexyl-2-aminoethanesulfonic acid (CHES, pH 9.2) at a final concentration of 20 mM. Each reaction was performed in the presence of 0.5 mM NAD(P), 1.0 mM phosphite, and 2.0  $\mu\text{g}/\text{mL}$  of protein at 37°C for 10 min. The NAD(P)H production was measured as described above.

### 3.2.7 SA Production and Detection

NADPH regeneration system using RsPtxD was utilized for 3-DHS conversion to SA by SDH. The coupling reaction of SDH and RsPtxD was performed in a solution containing 3-DHS, NADP, phosphite, SDH, and RsPtxD in 100 mM HEPES (pH 8.0). The reaction solutions with the final

volume of 500  $\mu\text{L}$  were incubated at 45°C. Fifty-microliter aliquots were periodically removed from the reaction solution and mixed with an equal volume of 20 mM glycine buffer (pH 2.0) to terminate the reaction. The conversion of 3-DHS to SA was monitored with an HPLC system (Jasco, Tokyo, Japan) equipped with a UV detector and column TSKgel ODS-80T<sub>M</sub> (250 mm  $\times$  4.6 mm internal diameter, and particle size; 5  $\mu\text{m}$ , Tosoh). An isocratic mixture of water/0.1 M H<sub>3</sub>PO<sub>4</sub> buffer (95:5 v/v) at a flow rate of 0.5 mL min<sup>-1</sup> was used to separate SA and 3-DHS, with concentrations measured spectrophotometrically at 230 nm. In this system, the retention times for SA and 3-DHS were detected at approximately 9.4 and 13.8 min, respectively.

### 3.3 Results

#### 3.3.1 Construction of RsPtxD mutants

Nicotinamide cofactors are engaged to a nucleotide-binding motif. The Rossman fold consists of two  $\alpha$ -helices and three  $\beta$ -strands in NAD(P)-dependent dehydrogenases. Binding the 2'-hydroxyl of adenine ribose where the phosphate group is occupied in NADP with the amino acids after the second  $\beta$ -strand of dehydrogenase determines their cofactor specificity (88). As a result, the electrostatic state of the amino acid side chains in this location is frequently a determinant of ligand binding and hence of nicotinamide substrate specificity (89). In numerous NAD-dependent dehydrogenases, substituting the amino acid residues in this region with basic amino acids lead to higher NADP affinity, whereas acidic amino acids replacement resulted in enhanced affinity for NAD (90). The alignment of amino acid-sequence of RsPtxD and PsePtxD exhibited that the amino acid residues placed at the C-terminus of the second  $\beta$ -strand (denoted as  $\beta$ 7 in Figure 3.1) in the Rossman-fold domain of RsPtxD were acidic aspartate at 175 and neutral proline at 176 (Figure 3.1), probably producing electrostatic repulsion against 2'-phosphate of NADP. Therefore, I substituted them with alanine and arginine, like those in a previous study (84). I also changed the surrounding three amino acids (Cys174, Ile177, and Pro178), which might be considered to influence the nicotinamide cofactor binding. Thus, I generated four mutants using site-directed mutagenesis with amino acids replacement, RsPtxD<sub>AR</sub> (D175A/P176R), RsPtxD<sub>HAR</sub> (C174H/D175A/P176R), RsPtxD<sub>HARKA</sub> (C174H/D175A/P176R/I177K/P178A), and RsPtxD<sub>HARRA</sub> (C174H/D175A/P176R/I177R/P178A) (Figure 3.1). All the mutant proteins were purified using a nickel-affinity column after being expressed in *E. coli*. I confirmed the enzyme's homogeneity using SDS-PAGE analysis of each purified protein with a molecular mass of 40.1 kDa.

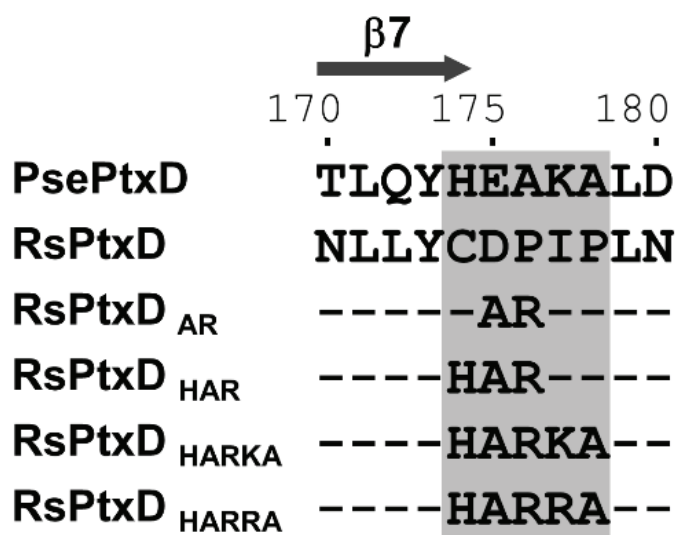


**Figure 3.1** The alignment of the amino acid sequences of PsePtxD, RsPtxD, and RsPtxD mutants. The mutations were introduced at the C-terminus region of the  $\beta 7$ -strand in the Rossman-fold domain (gray rectangle).

### 3.3.2 RsPtxD mutant's kinetic analysis

The RsPtxD mutants' kinetic values were evaluated under either NAD(P) or phosphite saturation conditions. The  $K_M$  for NAD ( $K_M^{\text{NAD}}$ ) and NADP ( $K_M^{\text{NADP}}$ ) of the wild-type RsPtxD showed  $7.7 \pm 2.3 \mu\text{M}$  and  $418 \pm 38.7 \mu\text{M}$ , respectively, verifying its higher affinity with NAD and poor binding with NADP as a cofactor (Table 3.2). As anticipated, the D175A/P176R mutations in RsPtxD (RsPtxD<sub>AR</sub>) resulted in a considerable reduction in  $K_M^{\text{NADP}}$  to  $56 \pm 5.1 \mu\text{M}$ , demonstrating that RsPtxD<sub>AR</sub> mutant has higher affinity for NADP than the wild-type enzyme. The insertion of the non-polar alanine at residue 175, which neutralizes the negative charge of the aspartate residue, and the basic arginine at position 176, generating a positively charged region that can accept the 2'-phosphate group of NADP, are likely responsible for the improved affinity for NADP. However, the catalytic efficiency ( $k_{\text{cat}}/K_M$ )<sup>NADP</sup> of RsPtxD<sub>AR</sub> was almost 20-fold lower than that of a PsePtxD mutant with the same amino acid substitutions (PsePtxD<sub>E175A/A176R</sub>) (Table 3.2, Table 3.3). When the amino acid sequences of PsePtxD and RsPtxD were compared, it was shown that the basic amino acids histidine and lysine were originally present at 174 and 177, respectively, in PsePtxD, while the neutral amino acids cysteine and isoleucine were occupied at the corresponding positions of RsPtxD (Figure 3.1). As a result, i hypothesized that the adjacent residues Cys174, Ile177, and Pro178 were responsible for the higher NADP catalytic efficiency of PsePtxD<sub>E175A/A176R</sub>. Indeed, when the C174H mutation was inserted into RsPtxD<sub>AR</sub> (RsPtxD<sub>HAR</sub>),  $K_M^{\text{NADP}}$  was lowered by  $24 \pm 5.2 \mu\text{M}$  with a slightly improved  $k_{\text{cat}}$ . Moreover, RsPtxD<sub>HARKA</sub> exhibited  $K_M^{\text{NADP}}$  values of  $4.4 \pm 0.9 \mu\text{M}$ , demonstrating that introducing I177K and P178A mutations to RsPtxD<sub>HAR</sub> may provide a synergetic influence in decreasing  $K_M^{\text{NADP}}$ . Based on this result, instead of lysine, i substituted isoleucine at 177 with the more basic arginine residue. The

generated mutant, RsPtxD<sub>HARRA</sub>, revealed the lowest  $K_M^{\text{NADP}}$  value of  $2.9 \pm 0.5 \mu\text{M}$  and best catalytic efficiency  $(k_{\text{cat}}/K_M)^{\text{NADP}}$  of  $44.1 \mu\text{M}^{-1} \text{min}^{-1}$  among all created mutants

**Table 3.2** The kinetic parameters of wild-type RsPtxD and its mutants<sup>a</sup>

Enzyme	NAD			NADP					
	$K_M$ ( $\mu\text{M}$ )	$k_{\text{cat}}$ ( $\text{min}^{-1}$ )	$k_{\text{cat}}/K_M$ ( $\mu\text{M}^{-1}\text{min}^{-1}$ )	$K_M$ ( $\mu\text{M}$ , Pt)	$k_{\text{cat}}$ ( $\text{min}^{-1}$ )	$k_{\text{cat}}/K_M$ ( $\mu\text{M}^{-1}\text{min}^{-1}$ )	$K_M$ ( $\mu\text{M}$ , Pt)	CSR <sup>b</sup>	RCE <sup>c</sup>
RsPtxD	7.7 ± 2.3	127 ± 16.8	16.6	37.0 ± 7.0	418 ± 38.7	4.0 × 10 <sup>-2</sup>	338 ± 41.0	2.3 × 10 <sup>-3</sup>	
RsPtxD <sub>AR</sub>	412 ± 21.5	115 ± 13.0	0.3	452 ± 16.1	56 ± 5.1	91.1 ± 3.9	263 ± 16.4	6.0	0.1
RsPtxD <sub>HAR</sub>	154 ± 14.7	155 ± 2.3	1.0	419 ± 89.9	24 ± 5.2	118 ± 6.8	208 ± 6.2	5.0	0.3
RsPtxD <sub>HARKA</sub>	130 ± 10.6	154 ± 7.5	1.2	388 ± 46.6	4.4 ± 0.9	129 ± 12.1	27 ± 9.0	25.0	1.8
RsPtxD <sub>HARRA</sub>	112 ± 1.3	148 ± 14.8	1.3	414 ± 45.8	2.9 ± 0.5	128 ± 16.6	38 ± 8.5	34.0	2.7

a. All assays were performed three times at 37°C, pH 7.3, in 100 mM MOPS. b. Cofactor Specificity Ratio =  $(k_{\text{cat}}/K_M)^{\text{NADP}} / (k_{\text{cat}}/K_M)^{\text{NAD}}$

c. Relative Catalytic Efficiency =  $(k_{\text{cat}}/K_M)^{\text{NADP}}_{\text{mut}} / (k_{\text{cat}}/K_M)^{\text{NAD}}_{\text{wt}}$ .

### 3.3.3 Optimal temperature, thermostability, and organic solvent tolerance of RsPtxD variants

To determine the optimum temperature of the RsPtxD mutants, i carried out enzyme assays at several temperatures ranging from 30°C to 60°C (Figure 3.2). In the presence of NAD cofactor, the wild-type RsPtxD exhibited the maximum activity at 50°C. The optimum temperature for RsPtxD<sub>AR</sub> and RsPtxD<sub>HAR</sub> was found to be 30°C to 40°C with NAD and 40°C with NADP, implying that D175A/P176R mutations decreased the optimal temperature while improving NADP affinity (Table 3.2). However, remarkably, the further mutations of I177K/P178A or I177R/P178A to RsPtxD<sub>HAR</sub> reestablished the optimal temperature with NADP to 50°C (Figure 3.2). Thereafter, the thermostability of the RsPtxD mutants was evaluated in the presence or absence of cofactor binding at 45°C. In the absence of a cofactor, the thermostabilities of all RsPtxD variants reduced dramatically (Figure 3.3A). However, preincubating RsPtxD<sub>AR</sub> or RsPtxD<sub>HAR</sub> with 0.5 mM NADP but not 0.5 mM NAD, marginally enhanced their thermostability (Figure 3.3A). At the same time, preincubation of RsPtxD<sub>HARKA</sub> and RsPtxD<sub>HARRA</sub> with 0.5 mM NADP but not 0.5 mM NAD substantially improved their thermostabilities over 6 hours (Figure 3.3A).

The author hypothesized that the protective effect of ligand binding on the RsPtxD mutants would also improve their stability in organic solvents due to thermotolerant enzymes are usually exhibit tolerant to organic solvents. When RsPtxD proteins were preincubated with or without NAD before being incubating at various concentrations of DMF, all the mutants lost their activity after 6 hours at 30% DMF (Figure 3.3B). When the RsPtxD mutants were preincubated with NADP, however, RsPtxD<sub>HARKA</sub> and RsPtxD<sub>HARRA</sub> displayed about 90% of the residual activities in 30% DMF. With RsPtxD<sub>AR</sub> and RsPtxD<sub>HAR</sub> mutants, the protective effect of NADP-binding was not observed. As a result, these findings strongly suggesting that robust cofactor binding

improves the resistance for organic solvents the mutant proteins, i.e., RsPtxD<sub>HARKA</sub> and RsPtxD<sub>HARRA</sub>.

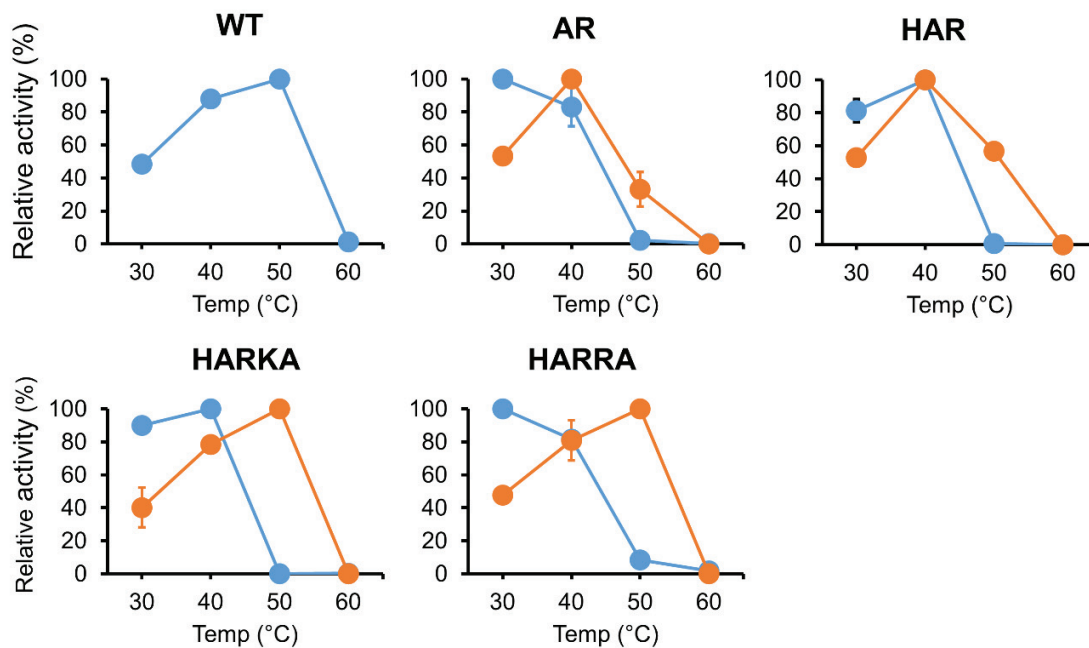


**Figure 3.2** The temperature dependence profiles of the wild-type and mutant RsPtxD proteins. Each protein's activity was measured using NAD (blue circles) or NADP (orange circles) as a nicotinamide cofactor. The data are shown as means  $\pm$  standard deviation obtained from three independent experiments. WT, wild-type. AR, RsPtxD<sub>AR</sub>. HAR, RsPtxD<sub>HAR</sub>. HARKA, RsPtxD<sub>HARKA</sub>. HARRA, RsPtxD<sub>HARRA</sub>.

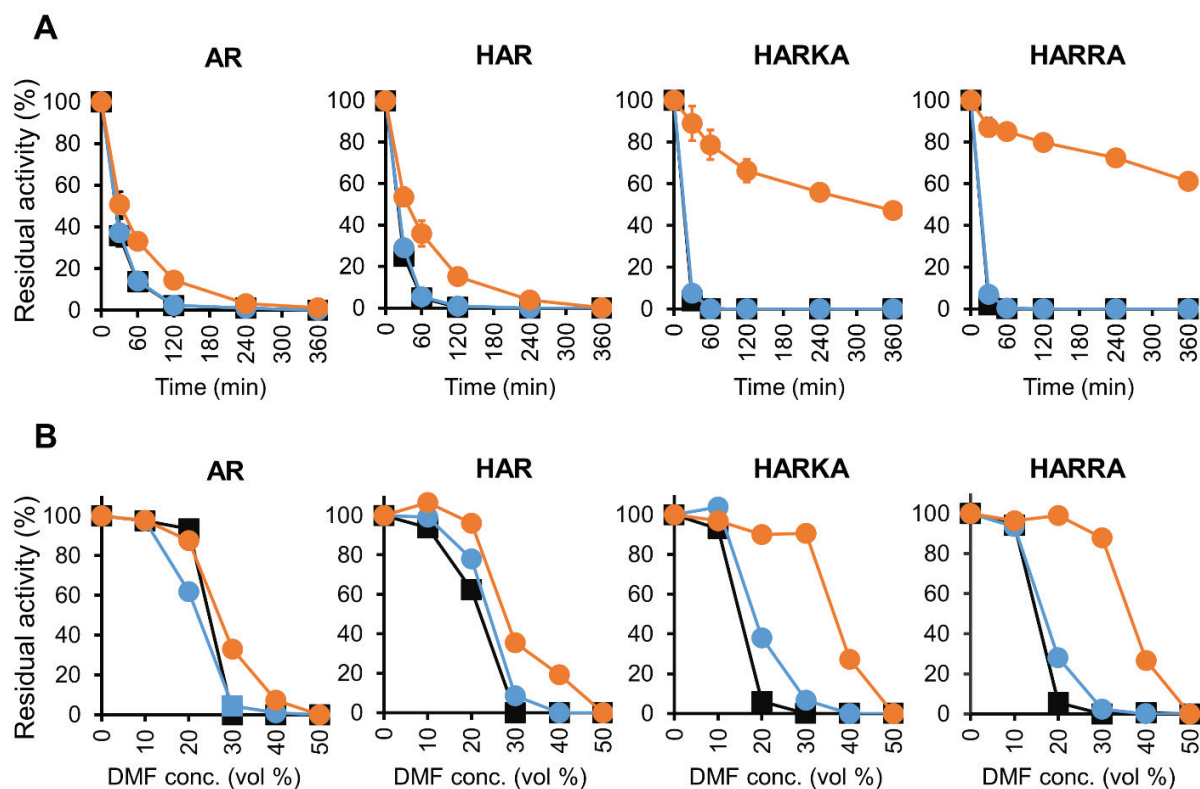


**Figure 3.3** Characterization of the thermal stability and tolerance to organic solvents for RsPtxD variants. **(A)** Thermal inactivation of RsPtxD mutants at 45°C. Data are presented as the mean  $\pm$  standard deviation from three experiments. **(B)** Stabilities of RsPtxD mutants in DMF. Prior to the assay reaction, RsPtxD mutants were incubated in the 50 mM MOPS (pH7.3) containing 0.5 mM NAD (blue circles), 0.5 mM NADP (orange circles), or without cofactor (squares). The reactions were performed by using 0.5 mM NADP as a nicotinamide substrate. The data are representative of two independent experiments. WT, wild-type. AR, RsPtxD<sub>AR</sub>. HAR, RsPtxD<sub>HAR</sub>. HARKA, RsPtxD<sub>HARKA</sub>. HARRA, RsPtxD<sub>HARRA</sub>.

### 3.3.4 The optimal pH of RsPtxD variants

The RsPtxD mutant's activity was further measured in the pH range of 6.2–9.2 (Figure 3.4). All of the RsPtxD mutants exhibited the maximum activity around pH 7.3 with NAD as a cofactor. Their activities reduced as pH increased, eventually disappearing at pH 9.2, whereas the wild-type RsPtxD kept more than 80% of its activity (Figure 3.4). When NADP was utilized as a cofactor, the activities of RsPtxD<sub>AR</sub> and RsPtxD<sub>HAR</sub> were maximum between pH 7.3 and 8.0; however, their activities at pH 9.2 dropped to around 20% (Figure 3.4). On the other hand, the optimal pH for RsPtxD<sub>HARKA</sub> and RsPtxD<sub>HARRA</sub> shifted substantially to a higher range (Figure 3.4). These findings suggest that the higher affinity of RsPtxD<sub>HARKA</sub> and RsPtxD<sub>HARRA</sub> toward NADP coupled with improved activity at higher pH levels.

### 3.3.5 Production of SA by utilizing RsPtxD as an NADPH generation system

To illustrate the ability of RsPtxD mutants as an NADPH regeneration system, RsPtxD proteins were paired with a thermostable SDH from *T. thermophilus* HB8 for SA production (Figure 3.5A). Using NADPH as a cofactor, SDH catalyzes the conversion of 3-DHS to SA, a precursor for the antiviral drug oseltamivir (Tamiflu<sup>®</sup>) (91). The substrate for the coupling reaction was 8 mM of 3-DHS in the presence of 0.1 mM NADP. At 45°C, the wild-type RsPtxD was unable to support SA production, indicating that it did not regenerate NADPH (Figure 3.5B). The reaction was sustained by RsPtxD<sub>AR</sub> for almost 28% of the substrate conversion; however, the reaction stopped after 30 minutes, possibly because of heat inactivation. On the other hand, RsPtxD<sub>HARRA</sub> enabled nearly complete conversion of 3-DHS to SA for 90 minutes, indicating that it regenerated NADPH without dropping its activity at 45°C. As a result, the SA production was around 22 g

$\text{L}^{-1}\text{d}^{-1}$  with a total turnover number (TTN) of 78. With additional amounts of substrate, 100 mM 3-DHS, a coupling reaction could produce  $61 \text{ g L}^{-1}\text{d}^{-1}$  with a TTN of 860 for NADPH.

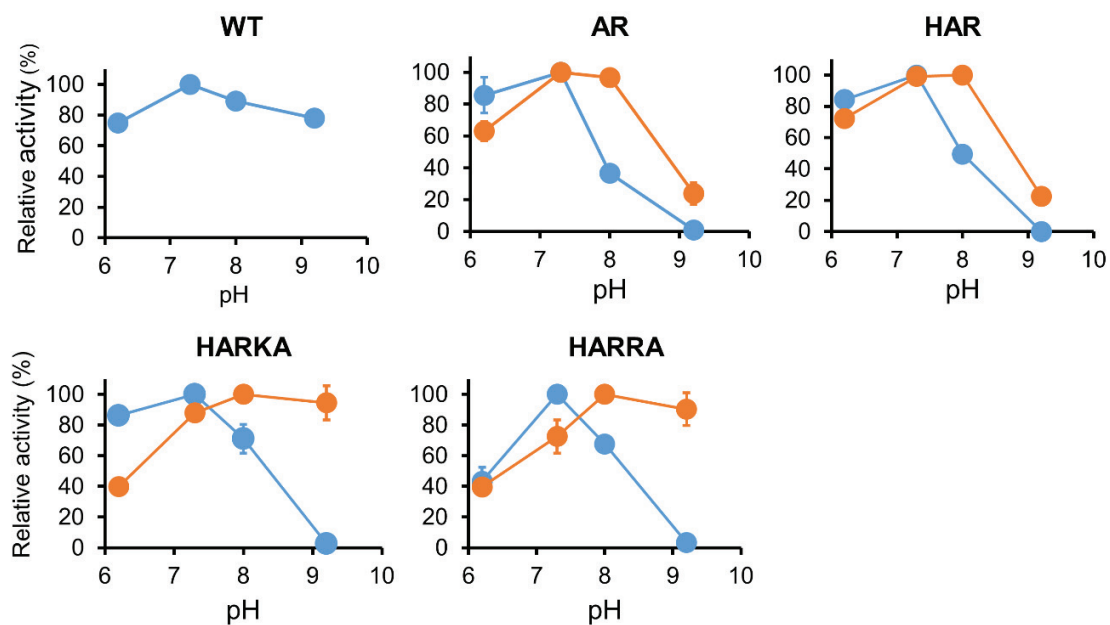


**Figure 3.4** pH dependence profiles of the wild-type and mutant RsPtxD proteins. RsPtxD activity was measured using NAD (blue circles) or NADP (orange circles) as substrates. The data are shown as means  $\pm$  standard deviation obtained from three independent experiments. WT, wild-type. AR, RsPtxD<sub>AR</sub>. HAR, RsPtxD<sub>HAR</sub>. HARKA, RsPtxD<sub>HARKA</sub>. HARRA, RsPtxD<sub>HARRA</sub>.

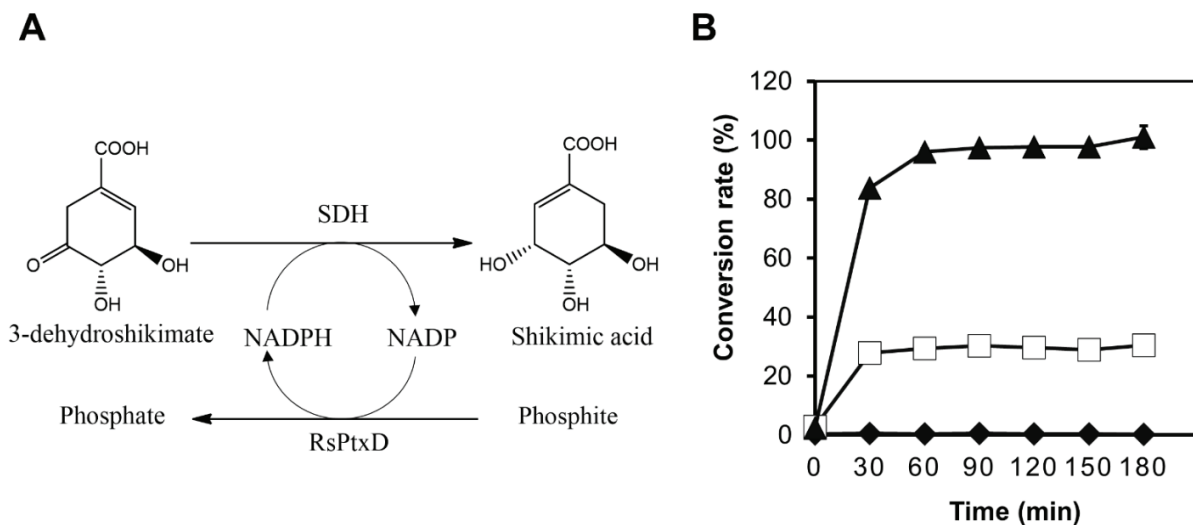


**Figure 3.5** Shikimic acid (SA) production by shikimate dehydrogenase with NADPH regeneration by RsPtxD. **(A)** A schematic of the coupled reactions of SA production by shikimate dehydrogenase (SDH) and NADPH regeneration by RsPtxD. **(B)** The batch production of SA from 3-dehydroshikimate by SDH with NADPH regeneration by wild-type RsPtxD (diamonds), RsPtxD<sub>AR</sub> (squares), and RsPtxD<sub>HARRA</sub> (triangles). The reaction solutions contained 20 mM phosphite, 8 mM 3-DHS, 0.1 mM NADP, 0.17 U/mL of SDH, and 20  $\mu$ g/mL of RsPtxD proteins.

## 3.4 Discussion

### 3.4.1 RsPtxD mutants with higher affinity toward NADP

The alteration of dehydrogenases' NAD(P) cofactor specificity is critical for the development of industrial biocatalysts. Because NADPH is so expensive, huge efforts have been made to switch the cofactor specificity of NADH-regenerative enzymes from NAD to NADP. In this part of our study, the cofactor specificity of a thermostable PtxD isolated from the soil bacterium *Ralstonia* sp. 4506 (RsPtxD) has been relaxed by substituting five residues, Cys174, Asp175, Pro176, Ile177, and Pro178, placed at the C-terminus of the  $\beta$ 7-strand region that engaged with the adenosine ribose moiety of a nicotinamide cofactor. RsPtxD mutant enzymes improved specificity and catalytic efficiency toward NADP while also being resistant to high temperatures and organic solvents. An increased of PsePtxD cofactor specificity to NADP previously reported by substituting Glu175 and Ala176 with Ala and Arg, respectively (PsePtxD<sub>E175A/A176R</sub>) (Woodyer et al., 2003). I noticed that changing the equivalent amino acids in RsPtxD (RsPtxD<sub>AR</sub>) substantially reduced the  $K_M$  for NADP, indicating substitutions of that amino acid at this region, especially from acidic to basic, was crucial in relaxing cofactor specificity. However, RsPtxD<sub>AR</sub> still had higher  $K_M$  for NADP than PsePtxD<sub>E175A/A176R</sub> (Table 3.2, 3.3). The further mutations in RsPtxD<sub>AR</sub> at Cys174His, Ile177Lys, and Pro178Ala, generated RsPtxD<sub>HARKA</sub>, which has a lower  $K_M$  for NADP attributed to higher catalytic efficiency. The best mutant, RsPtxD<sub>HARRA</sub>, was created by replacing Ile177 with Arg which exhibited the greatest catalytic efficiency of all mutants. These finding suggested that recognizing nicotinamide cofactors required not only Asp175 and Pro176, but also surrounding amino acid residues of RsPtxD. According to a molecular modeling investigation based on the RsPtxD structure (Protein Data Bank ID 6IH3, (92)), replacing Cys174 with His stabilized nicotinamide cofactors binding in RsPtxD<sub>AR</sub> by generating a more compact

binding pocket where the adenine moiety of NAD(P) could be adapted (Figure 3.6). The lowered  $K_{MS}$  of RsPtxD<sub>HAR</sub> for both NAD and NADP than those of RsPtxD<sub>AR</sub> is compatible with this modeling (Table 3.2). The  $K_M$  of RsPtxD<sub>HAR</sub> was further decreased by replacing Ile177 with Lys, probably by generating a positively charged surface at the entrance of the NAD(P)-binding pocket and stimulating NADP loading with appropriate direction of the 2'-phosphate group into the binding site. In the case of RsPtxD<sub>HARRA</sub>, introducing the more basic arginine instead of Ile177, resulted in increased hydrogen-bonding formation and ionic interactions with NADP (Figure 3.6). GBVI/WSA dG predicted protein-ligand affinity by calculating the ligand's binding free energy from a given pose (93,94). The strongest affinity was found in RsPtxD<sub>HARRA</sub>-NADP complex (−9.66 kcal/mol) after molecular modeling analysis of four RsPtxD mutants using this calculation tool (Figure 3.6).

### 3.4.2 The optimal pH shift of RsPtxD variants

For RsPtxD<sub>HARKA</sub> and RsPtxD<sub>HARRA</sub> mutants, where a positively charged amino acid residue, Ile177Lys and Ile177Arg, was inserted into the NADP-binding region, a substantial shift to higher pH was observed for maximum activity (Figure 3.4). Similarly, Zhang et al. found that the activity of wild-type alcohol dehydrogenase from *Vibrio harveyi* (Vh-ALDH) was reduced at a higher pH (pH 8-9), whereas all the activity for its mutants (Thr175Asp and Thr175Glu), whose cofactor specificity was switched from NADP to NAD, was improved in the same pH range (95). Surprisingly, they noticed that the  $K_M$  of Thr175Asp and Thr175Glu mutants at pH 9.0 for NAD increased around 10-fold compared with values at pH 8.0. Although the explanation for this mechanism was ambiguous, they revealed that the increase in these mutants' activity from pH 8.0 to 9.0 was mostly due to an increase in  $K_{cat}$ . As a result, the author tested the RsPtxD<sub>AR</sub> mutant's activity at higher NADP concentrations (1.0 mM and 1.5 mM). Consequently, the optimal pH of

RsPtxD<sub>AR</sub> moved from 7.3 to 8.0, while the relative activity at pH 9.2 increased to around 55% and 70% of the maximal activity in the reactions containing 1.0 mM and 1.5 mM NADP, respectively (Figure 3.7A). These findings clearly indicated that the lower relative activity of RsPtxD<sub>AR</sub> at pH 9.2 was mostly likely caused by the lower  $K_M$ , which might be compensated by the increased NADP concentration. As initially stated, higher affinities of RsPtxD<sub>HARKA</sub> and RsPtxD<sub>HARRA</sub> with NADP may help with the high relative activity at high pH (~90% of the maximum activity at pH 9.2, Figure 3.4).

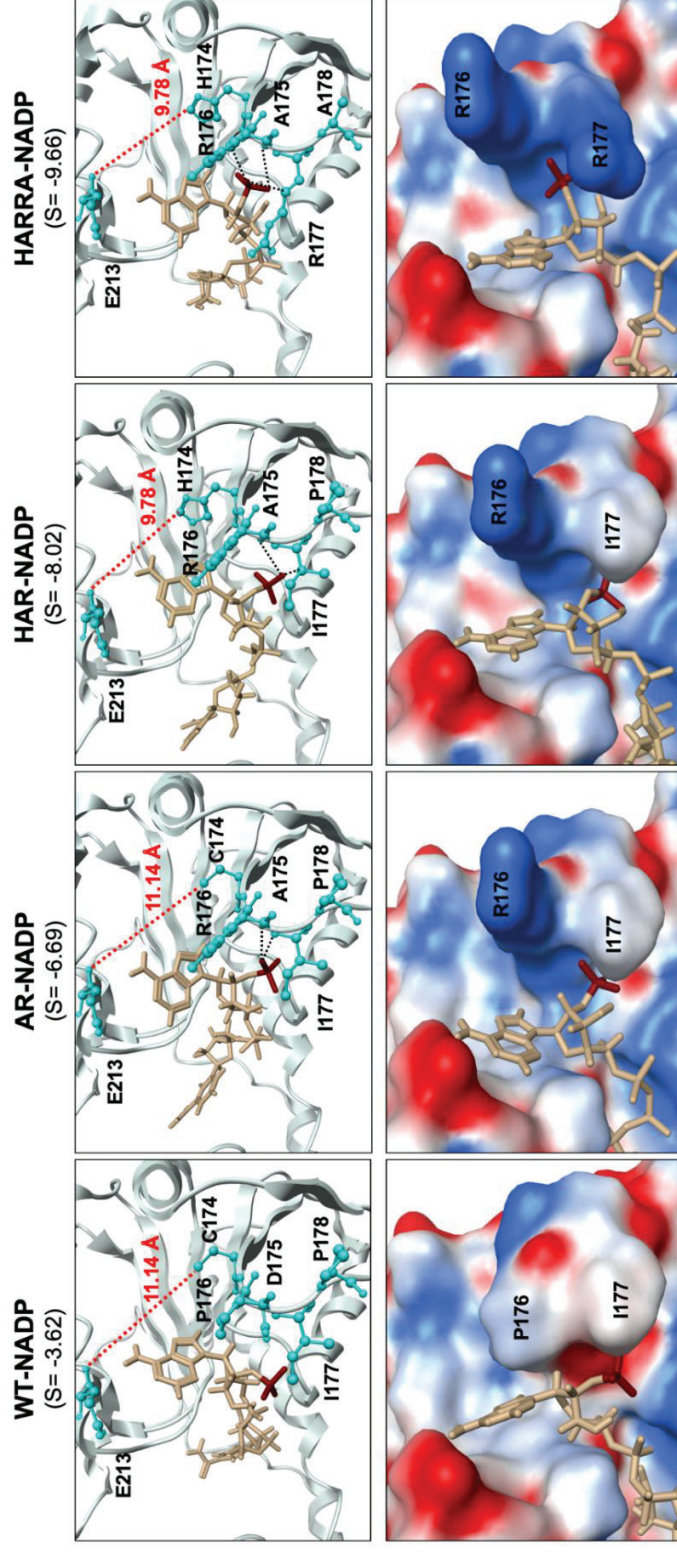


**Figure 3.6.** Proposed model structures of the NAD-binding pocket of RsPtxD (WT), RsPtxD<sub>AR</sub> (AR), RsPtxD<sub>HAR</sub> (HAR), and RsPtxD<sub>HARRA</sub> (HARRA) (Top panels). The side chains of amino acid residues at 174, 175, 176, 177, 178, and 213 are shown in cyan. The protein structures were modeled by the Molecular Operating Environment software (MOE; Chemical Computing Group Inc., Montreal, Canada) using the PDB 6IH3 structure (92) as a template. The distance between the residues at 174 and 213 was shown with a red dotted line. The NAD moiety was shown in light brown and the 2'-phosphate group was shown in dark red. Note that the distances between the residues 174 and 213 in RsPtxD<sub>HAR</sub> and RsPtxD<sub>HARRA</sub> are shorter than that in RsPtxD and RsPtxD<sub>AR</sub>. Hydrogen bonding between residues and cofactor were shown as black dotted lines. The numbers (S values) in the parenthesis are binding energy (kcal/mol) of NADP and RsPtxDs calculated by the GBVI/WSA dG scoring function of the MOE software. The electrostatic surface potentials of the proposed model structures of the NAD-binding pocket of RsPtxD and its mutants (Bottom panels). Positively charged region is indicated in blue and negatively charged region in red.

### 3.4.3 Thermostability and solvent stability are improved by higher NADP affinity of RsPtxD variants

Thermostability experiments revealed that NADP binding protected RsPtxD<sub>HARKA</sub> and RsPtxD<sub>HARRA</sub> against heat treatment at 45°C, but not RsPtxD<sub>AR</sub> and RsPtxD<sub>HAR</sub>. Even after heat treatment for six hours, RsPtxD<sub>HARRA</sub> retained around 60% of its activity after preincubation with 0.5 mM NADP. At the same temperature, RsPtxD<sub>HARRA</sub> preincubated with NAD lost its activity within an hour. During the thermal stability assay, I further noticed that the low affinity of RsPtxD<sub>AR</sub> can be compensated by an increased concentration of NADP (1.5 mM) (Figure 3.7B). These findings revealed that a direct correlation between the thermal protection effect and the NADP binding affinity of RsPtxD mutants. Similar thermal protection effects of NAD(P) ligand-binding to enzymes have been found in PsePtxD (84), aldehyde dehydrogenase of *V. harveyi* (95), and a glyceraldehyde-3-phosphate dehydrogenase of *Bacillus stearothermophilus* (96). In all cases, binding with the preferred nicotinamide cofactor protects the enzyme against thermal inactivation, but binding with lower affinity cofactor affords little or no protection. As described earlier, because of the increased hydrogen-bonding formation and ionic interactions, RsPtxD<sub>HARRA</sub> exhibited a higher affinity for NADP. As reported in several studies, high ligand binding improved protein thermostability by coupling the binding with unfolding equilibrium (97-99). As a result, the higher thermostability of RsPtxD<sub>HARRA</sub> mutant enzyme is likely due to the increased affinity to NADP. This ligand binding stabilizing effect could also be attributed to the NADP-bound RsPtxD<sub>HARRA</sub> tolerance of organic solvents. Because conducting industrial enzymatic reactions in organic solvents has several advantages, including increased solubility of organic substrates (100), the higher organic solvent stability of RsPtxD<sub>HARRA</sub> as well as improved thermostability further expanded the potential applications of PtxD enzymes.

According to Relyea et al, the PtxD reaction is an ordered bi-bi mechanism in which the substrates NAD bind first then phosphite, and the products phosphate is released first, then NADH (101). In this model, NAD binding causes a conformational change in PtxD, which allow access to the phosphite binding pocket. This was consistent with our findings that when the affinity of RsPtxD mutants for NADP increased, their phosphite affinity also increased. This model was further supported by the reverse effects when NAD was utilized as a cofactor (Table 3.2). Overall, higher NADP-binding with RsPtxD<sub>HARRA</sub> attributed to improved heat stability and solvent stability, as well as phosphite affinity.

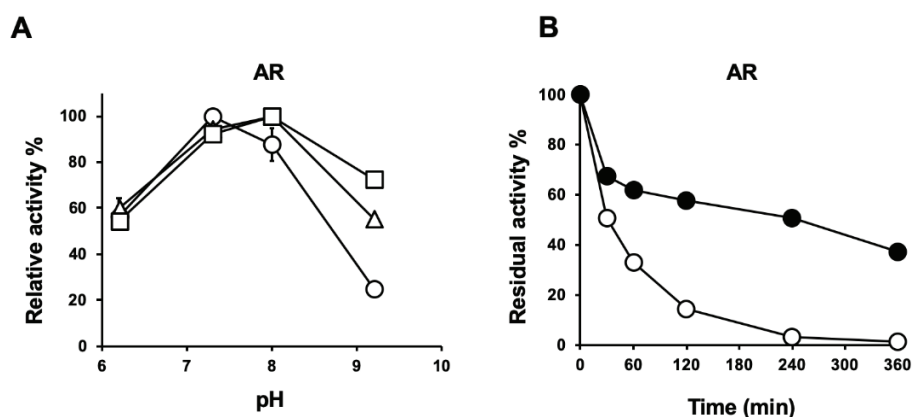


**Figure 3.7** pH dependent profile (A) and thermal stability (B) of RsPtxD<sub>AR</sub> mutant (AR). (A) PtxD activity was measured using 0.5 mM (circles), 1.0 mM (triangles), and 1.5 mM (squares) of NADP. The data are shown as means  $\pm$  standard deviation obtained from three independent experiments. (B) Thermal inactivation of RsPtxD<sub>AR</sub> was performed with 0.5 mM (open circles) and 1.5 mM (closed circles). The data was representative of two independent experiments, with essentially the same results.

### 3.4.4 Comparisons with other research studies for cofactor switching and improvements in NADP-regeneration enzymes

Recently, a comprehensive review summarized the findings of 52 NAD-dependent enzymes whose cofactor specificity switched from NAD to NADP, 30% of which resulted in variants with catalytic efficiency toward NADP better than the catalytic efficiency of the wild-type enzymes with their natural cofactor, NAD (Relative Catalytic Efficiency, RCE > 1.0) (90). In our study, RsPtxD<sub>HARRA</sub> revealed its RCE value of 2.7 (Table 3.2), suggesting that the catalytic efficiency with NADP was substantially superior compared with that of wild-type RsPtxD with NAD. The coenzyme specificity ratio (CSR) determines the changes in the preference ratio of the target cofactor in the mutant enzyme. The CSRs of RsPtxD and RsPtxD<sub>HARRA</sub> were  $2.3 \times 10^{-3}$  and 34.0, respectively, indicating modifications of the amino acid residues contacting the 2'-position of NAD and the residues in the surrounding positions were both important in altering the preference for target cofactors.

As mentioned in the introduction, FDH is one of the most widely used NADPH regenerative enzymes (103). Recently, various attempts have been made to improve the catalytic efficiency of FDH for NADP; two of the most recent attempts have been successful. By structural modeling analysis, Jiang et al. enhanced the catalytic efficiency of the FDH from *Burkholderia stabilis* 15516 to around  $5.9 \mu\text{M}^{-1} \text{min}^{-1}$  (101). Calzadiaz-Ramirez et al., performing *in vivo* selection with an *E. coli* host that was an auxotrophic to NADPH, identified an FDH mutant from *Pseudomonas* sp. 101 (PseFDH-V9) that exhibited catalytic efficiency of around  $8.5 \mu\text{M}^{-1} \text{min}^{-1}$ , which was the best value among the previously informed FDHs (102). Despite the fact that both enzymes exhibited relatively high  $K_{\text{cat}}$  values, their catalytic efficiencies are around 5–7 times lower than that of RsPtxD<sub>HARRA</sub>. Moreover, due to their high  $K_{\text{M}}$  for formate (9–31 mM), FDHs

require a high substrate concentration (Table 3.3). RsPtxD<sub>HARRA</sub>, on the other hand, exhibited low  $K_{MS}$  for both NADP and phosphite, indicating that the amount of required substrates can be decreased without impacting its maximal activity.

**Table 3.3** Comparison of kinetic parameters of NADP-dependent enzymes previously reported

Enzyme	NADP				Assay conditions	References
	$K_M$ ( $\mu\text{M}$ , NADP)	$K_{\text{cat}}$ ( $\text{min}^{-1}$ )	$K_{\text{cat}}/K_M$ ( $\mu\text{M}^{-1}$ $\text{min}^{-1}$ )	$K_M$ ( $\mu\text{M}$ , Pt or formate)		
PsePtxD <sub>E175A/A176R</sub>	$3.5 \pm 0.5$	$114 \pm 33.0$	32.5	$21 \pm 3.0$	25 °C, pH 7.25	(84)
PsePtxD <sub>12x-A176R</sub>	$5.5 \pm 0.7$	$82 \pm 4.0$	14.9	$36 \pm 14.0$	25 °C, pH 7.25	(85)
mut PseFDH	$150 \pm 25$	$150 \pm 9.0$	1.0	$9000 \pm 3000$	30 °C, pH 7.0	(103)
BstFDH <sub>G146M/A287G</sub>	$90 \pm 0.0$	$529 \pm 1.8$	5.9	$31700 \pm 3700$	30 °C, pH 7.0	(101)
PseFDH-V9	$26 \pm 1.0$	$221 \pm 1.8$	8.5	$24000 \pm 2400$	30 °C, pH 7.0	(102)

## **Chapter 4**

### **General conclusion**

Phosphite dehydrogenase (PtxD), is an NAD-dependent oxidoreductase, which catalyzes the oxidation of Pt to Pi, with a concomitant reduction of NAD to NADH. In addition to Pt being a nonmetabolizable form for the vast majority of organisms and is rare in the environment, the discovery of RsPtxD enzyme with high catalytic activity and thermostability, facilitated the development of several novel biotechnological applications. These applications include (i) an effective NADH regeneration system to produce chiral compounds by dehydrogenases, (ii) a dominant selective cultivation system for microorganisms and plants, and (iii) a biological containment strategy for ensuring biosafety and reducing the risk of contamination of genetically modified organisms. However, the currently available PtxD enzymes are NAD-dependent, making these applications unfeasible or less effective.

With these in mind, in this study the author aimed to boarder the biotechnological applications of the RsPtxD enzyme. For *in vivo* applications by achieving the biocontainment strategy of *Syn 7942* based on Pt dependency. For *in vitro* applications via engineering the cofactor specificity of RsPtxD for an effective NADPH regeneration system, both of which are required for industrial applications.

In chapter 2, the author successfully implemented a biological containment strategy based on Pt dependency to the model cyanobacterium *Synechococcus elongatus* PCC 7942 (*Syn 7942*) that was previously established in heterotrophic bacteria *E.coli*. Heterologous expression of RsPtxD and hypophosphite transporter (HtxBCDE) genes that allow the selective uptake of Pt, but not Pi, as well as disrupting all the indigenous Pi transporter genes, resulted in a strain which can grow only on Pt-containing media, and quickly lost viability in the absence of Pt. Moreover, the Pt-dependent strain could outcompete competitor cyanobacteria strains in the medium containing Pt. As a result, due to the scarcity of Pt in aquatic environments, this strategy may contribute to both

biosafety and contamination management of genetically engineered cyanobacteria in practical applications.

In chapter 3, by substituting the five amino acid residues, Cys174–Pro178, located at the C-terminus of the  $\beta$ 7-strand in the Rossmann-fold domain, I am able to engineer the cofactor specificity of RsPtxD toward NADP, achieving the best kinetic parameters ever reported for PtxD enzymes with NADP. Moreover, preincubation of RsPtxD<sub>HARRA</sub> mutant in the presence of 0.5 mM NADP exhibited protection from thermal inactivation at 45°C for up to 6 h and high tolerance to organic solvents. The author further confirmed the ability of RsPtxD<sub>HARRA</sub> as an effective NADPH regeneration system in the coupled reaction of chiral conversion of 3-DHS to SA by the thermophilic shikimate dehydrogenase of *Thermus thermophilus* HB8 at 45°C, which are difficult to achieve using the wild-type RsPtxD. Considering these properties of the RsPtxD mutants, the higher affinity toward NADP makes them especially promising for *in vitro* NADPH regeneration systems, which contribute to overcoming the cofactor challenge of NADP-dependent enzymes for industrial applications.

For *in vivo* applications, the author successfully expanded the host cell range of Pt-biological containment from heterotrophic bacterium *E.coli* to photosynthetic bacterium cyanobacteria. The genetic modification for P metabolic engineering in this system is simple and easy, meaning it may guide us to implement our Pt-dependent strategy to various bacteria beyond the types of the species. For instance, novel microalgae and cyanobacterial strains with tolerance to elevated temperatures, higher salts, and CO<sub>2</sub> concentrations have been recently isolated and have a promising commercial application in non-arable lands such as the Arabian desert. However, their inability to grow under industrially relevant outdoor conditions limits large scale application. Thus, by applying our strategy, it might make them promising hosts on an industrial scale in a sustainable process without

competing for land plants. However, the lowered growth of the Pt-dependent strain still challenges should be addressed before expanding our strategy.

As stated in chapter 2, i initially hypothesized that the use of the wild-type RsPtxD for biological containment of cyanobacteria might cause a NADH/NAD imbalance in the cell, thereby reducing the growth of Pt-dependent strain. In contrast to heterotrophic bacteria, NADP(H) is more abundant in photosynthetic bacteria (104). To address such a limitation, the author recently introduced RsPtxD<sub>HARRA</sub> created into *Syn 7942*, hopefully to obtain optimal redox balances and overcome this challenge. However, the preliminary result revealed that RsPtxD<sub>HARRA</sub> cannot recover the reduced cell growth on Pt. Therefore, only the redox balance due to RsPtxD enzyme cannot account for the growth differences between the strains. Other reasons for reduced growth, probably the lowered Pt affinity of HtxB or PtxD activity, which both reduce the phosphorus flux, resulted in growth retardation. Thus, maintaining maximal phosphorus flux by improving the Pt affinity of HtxB protein or looking for other PtxD enzyme from different species with higher activity may restore growth retardation in genetically modified strain.

In conclusion, this work expanded the *in vivo* and *in vitro* practical applications of RsPtxD. The development of a biocontainment strategy based on Pt, which can be easily applied to other organisms, thereby opening the way to use genetically modified microorganisms in open environments without consideration of biosafety and contamination risks. Moreover, engineering the cofactor specificity of RsPtxD toward NADP will expand the enzymatic toolbox available for biocatalysis and overcome cofactor challenges for NADP-dependent enzymes.

## References

1. **Metcalf, W. W., and Wolfe, R. S. (1998).** Molecular genetic analysis of phosphite and hypophosphite oxidation by *Pseudomonas stutzeri* WM88. *J. Bacteriol.* 180, 5547-5558.
2. **White, A. K., and Metcalf, W. W. (2002).** Isolation and biochemical characterization of hypophosphite/2-oxoglutarate dioxygenase. A novel phosphorus-oxidizing enzyme from *Pseudomonas stutzeri* WM88. *J. Biol. Chem.* 277, 38262-38271.
3. **Costas, A. M. G., White, A. K., and Metcalf, W. W. (2001).** Purification and characterization of a novel phosphorus-oxidizing enzyme from *Pseudomonas stutzeri* WM88. *J. Biol. Chem.* 276, 17429-17436.
4. **Kuroda, A., and Hirota, R. (2015).** Environmental biotechnology for efficient utilization of industrial phosphite waste. *Global. Environ. Res.* 19,77-82.
5. **Hirota, R., Yamane, S. T., Fujibuchi, T., Motomura, K., Ishida, T., Ikeda, T., and Kuroda, A. (2012).** Isolation and characterization of a soluble and thermostable phosphite dehydrogenase from *Ralstonia* sp. strain 4506. *J. Biosci. Bioeng.* 113, 445-450.
6. **Abed, R. M. M., Dobretsov, S., and Sudesh, K. (2009).** Applications of cyanobacteria in biotechnology. *J. Appl. Microbiol.* 106, 1-12.
7. **Smith, V. H., Sturm, B. S. M., deNoyelles, F. J., and Billings, S. A. (2010).** The ecology of algal biodiesel production. *Trends Ecol. Evol.* 25, 301-309.

8. **Moses, T., Mehrshahi, P., Smith, A. G., and Goossens, A. (2017).** Synthetic biology approaches for the production of plant metabolites in unicellular organisms. *J. Exp. Bot.* 68, 4057-4074.
9. **Mata, T. M., Martins, A. A., and Caetano, N. S. (2010).** Microalgae for biodiesel production and other applications: A review. *Renew. Sust. Energ. Rev.* 14, 217-232.
10. **Brueggeman, A. J., Kuehler, D., and Weeks, D. P. (2014).** Evaluation of three herbicide resistance genes for use in genetic transformations and for potential crop protection in algae production. *Plant Biotechnol. J.* 12, 894-902.
11. **Kumar, S. (2015).** GM algae for biofuel production: Biosafety and risk assessment. *Collect. Biosaf. Rev.* 9, 52-75.
12. **Berg, P., Baltimore, D., Brenner, S., Roblin, R. O., and Singer, M. F. (1975).** Summary statement of the Asilomar conference on recombinant DNA molecules. *Proc. Natl. Acad. Sci. U.S.A.* 72, 1981-1984.
13. **Wright, O., Delmans, M., Stan, G. B., and Ellis, T. (2015).** GeneGuard: A modular plasmid system designed for biosafety. *ACS Synth. Biol.* 4, 307-316.
14. **Molin, S., Boe, L., Jensen, L. B., Kristensen, C. S., Givskov, M., Ramos, J. L., and Bej, A. K. (1993).** Suicidal genetic elements and their use in biological containment of bacteria. *Annu. Rev. Microbiol.* 47, 139-166.
15. **Caliando, B. J., and Voigt, C. A. (2015).** Targeted DNA degradation using a CRISPR device stably carried in the host genome. *Nat. Commun.* 6, 6989.

16. **Celesnik, H., Tansek, A., Tahirovic, A., Vizintin, A., Mustar, J., Vidmar, V., and Dolinar, M. (2016).** Biosafety of biotechnologically important microalgae: intrinsic suicide switch implementation in cyanobacterium *Synechocystis* sp. PCC 6803. *Biol. Open* 5, 519-528.
17. **Rovner, A. J., Haimovich, A. D., Katz, S. R., Li, Z., Grome, M. W., Gassaway, B. M., Amiram, M., Patel, J. R., Gallagher, R. R., Rinehart, J., and Isaacs, F. J. (2015).** Recoded organisms engineered to depend on synthetic amino acids. *Nature* 518, 89-93.
18. **Mandell, D. J., Lajoie, M. J., Mee, M. T., Takeuchi, R., Kuznetsov, G., Norville, J. E., Gregg, C. J., Stoddard, B. L., and Church, G. M. (2015).** Biocontainment of genetically modified organisms by synthetic protein design. *Nature* 518, 55-60.
19. **Lopez, G., and Anderson, J. C. (2015).** Synthetic auxotrophs with ligand-dependent essential genes for a BL21(DE3) biosafety strain. *ACS Synth. Biol.* 4, 1279-1286.
20. **Van Mooy, B. A. S., Krupke, A., Dyhrman, S. T., Fredricks, H. F., Frischkorn, K. R., Ossolinski, J. E., Repeta, D. J., Rouco, M., Seewald, J. D., and Sylva, S. P. (2015).** Phosphorus cycling. Major role of planktonic phosphate reduction in the marine phosphorus redox cycle. *Science* 348, 783-785.
21. **White, A. K., and Metcalf, W. W. (2007).** Microbial metabolism of reduced phosphorus compounds. *Annu. Rev. Microbiol.* 61, 379-400.
22. **Morton, S. C., and Edwards, M. (2005).** Reduced phosphorus compounds in the environment. *Crit. Rev. Env. Sci. Tec.* 35, 333-364.

23. **Kanda, K., Ishida, T., Hirota, R., Ono, S., Motomura, K., Ikeda, T., Kitamura, K., and Kuroda, A. (2014).** Application of a phosphite dehydrogenase gene as a novel dominant selection marker for yeasts. *J. Biotechnol.* *182*, 68-73.
24. **Hirota, R., Motomura, K., and Kuroda, A. (2018).** Biological phosphite oxidation and its application to phosphorus recycling. In *Phosphorus recovery and recycling* (Ohtake, H., and Tsuneda, S., Eds.), p in press, Springer, Singapore.
25. **Loera-Quezada, M. M., Leyva-Gonzalez, M. A., Velazquez-Juarez, G., Sanchez-Calderon, L., Do Nascimento, M., Lopez-Arredondo, D., and Herrera-Estrella, L. (2016).** A novel genetic engineering platform for the effective management of biological contaminants for the production of microalgae. *Plant Biotechnol. J.* *14*, 2066-2076.
26. **Shaw, A. J., Lam, F. H., Hamilton, M., Consiglio, A., MacEwen, K., Brevnova, E. E., Greenhagen, E., LaTouf, W. G., South, C. R., van Dijken, H., and Stephanopoulos, G. (2016).** Metabolic engineering of microbial competitive advantage for industrial fermentation processes. *Science* *353*, 583-586.
27. **Hirota, R., Abe, K., Katsuura, Z. I., Noguchi, R., Moribe, S., Motomura, K., Ishida, T., Alexandrov, M., Funabashi, H., Ikeda, T., and Kuroda, A. (2017).** A novel biocontainment strategy makes bacterial growth and survival dependent on phosphite. *Sci. Rep.* *7*, 44748.
28. **Watanabe, S., Ohbayashi, R., Kanesaki, Y., Saito, N., Chibazakura, T., Soga, T., and Yoshikawa, H. (2015).** Intensive DNA replication and metabolism during the lag phase in cyanobacteria. *PLOS ONE* *10*, e0136800.

29. **Kuroda, A., Takiguchi, N., Gotanda, T., Nomura, K., Kato, J., Ikeda, T., and Ohtake, H. (2002).** A simple method to release polyphosphate from activated sludge for phosphorus reuse and recycling. *Biotechnol. Bioeng.* 78, 333-338.
30. **Bisson, C., Adams, N. B. P., Stevenson, B., Brindley, A. A., Polyviou, D., Bibby, T. S., Baker, P. J., Hunter, C. N., and Hitchcock, A. (2017).** The molecular basis of phosphite and hypophosphite recognition by ABC-transporters. *Nat. Commun.* 8, 1746.
31. **Falkner, R., Wagner, F., Aiba, H., and Falkner, G. (1998).** Phosphate-uptake behaviour of a mutant of *Synechococcus* sp. PCC 7942 lacking one protein of the high-affinity phosphate-uptake system. *Planta* 206, 461-465.
32. **Kobayashi, I., Watanabe, S., Kanesaki, Y., Shimada, T., Yoshikawa, H., and Tanaka, K. (2017).** Conserved two-component Hik34-Rre1 module directly activates heat-stress inducible transcription of major chaperone and other genes in *Synechococcus elongatus* PCC 7942. *Mol. Microbiol.* 104, 260-277.
33. **Frain, K. M., Gangl, D., Jones, A., Zedler, J. A. Z., and Robinson, C. (2016).** Protein translocation and thylakoid biogenesis in cyanobacteria. *Biochim. Biophys. Acta* 1857, 266-273.
34. **Barnett, J. P., Robinson, C., Scanlan, D. J., and Blindauer, C. A. (2011).** The Tat protein export pathway and its role in cyanobacterial metalloprotein biosynthesis. *FEMS Microbiol. Lett.* 325, 1-9.
35. **Higgins, C. F. (1992).** ABC transporters: from microorganisms to man. *Annu. Rev. Cell Biol.* 8, 67-113.

36. **Wagner, F., Falkner, R., and Falkner, G. (1995).** Information about previous phosphate fluctuations is stored via an adaptive response of the high-affinity phosphate uptake system of the cyanobacterium *Anacystis nidulans*. *Planta* 197, 147-155.
37. **Elser, J. J., Bracken, M. E. S., Cleland, E. E., Gruner, D. S., Harpole, W. S., Hillebrand, H., Ngai, J. T., Seabloom, E. W., Shurin, J. B., and Smith, J. E. (2007).** Global analysis of nitrogen and phosphorus limitation of primary producers in freshwater, marine and terrestrial ecosystems. *Ecol. Lett.* 10, 1135-1142.
38. **Wu, J. F., Sunda, W., Boyle, E. A., and Karl, D. M. (2000).** Phosphate depletion in the western North Atlantic Ocean. *Science* 289, 759-762.
39. **Kolowitz, L. C., Ingall, E. D., and Benner, R. (2001).** Composition and cycling of marine organic phosphorus. *Limnol. Oceanogr.* 46, 309-320.
40. **Lin, W., Zhao, D., and Luo, J. (2017).** Distribution of alkaline phosphatase genes in cyanobacteria and the role of alkaline phosphatase on the acquisition of phosphorus from dissolved organic phosphorus for cyanobacterial growth. *J. Appl. Phycol.* Epub Sep 21, 2017. DOI: 10.1007/s10811-017-1267-3.
41. **Ray, J. M., Bhaya, D., Block, M. A., and Grossman, A. R. (1991).** Isolation, transcription, and inactivation of the gene for an atypical alkaline phosphatase of *Synechococcus* sp. strain PCC 7942. *J. Bacteriol.* 173, 4297-4309.
42. **Wagner, K. U., Masepohl, B., and Pistorius, E. K. (1995).** The cyanobacterium *Synechococcus* sp. strain PCC 7942 contains a second alkaline phosphatase encoded by *phoV*. *Microbiology-UK* 141, 3049-3058.

43. **Suzuki, S., Ferjani, A., Suzuki, I., and Murata, N. (2004).** The SphS-SphR two component system is the exclusive sensor for the induction of gene expression in response to phosphate limitation in *Synechocystis*. *J. Biol. Chem.* 279, 13234-13240.
44. **Coupe, R. H., Kalkhoff, S. J., Capel, P. D., and Gregoire, C. (2012).** Fate and transport of glyphosate and aminomethylphosphonic acid in surface waters of agricultural basins. *Pest Manag. Sci.* 68, 16-30.
45. **Nanny, M. A., and Minear, R. A. (1997).** Characterization of soluble unreactive phosphorus using  $^{31}\text{P}$  nuclear magnetic resonance spectroscopy. *Mar. Geol.* 139, 77-94.
46. **Kutovaya, O. A., Mckay, R. M. L., and Bullerjahn, G. S. (2013).** Detection and expression of genes for phosphorus metabolism in picocyanobacteria from the Laurentian Great Lakes. *J. Great Lakes Res.* 39, 612-621.
47. **Yao, M. Y., Henny, C., and Maresca, J. A. (2016).** Freshwater bacteria release methane as a by-product of phosphorus acquisition. *Appl. Environ. Microbiol.* 82, 6994-7003.
48. **Clark, R. L., Gordon, G. C., Bennett, N. R., Lyu, H., Root, T. W., and Pflge, B. F. (2018).** High-CO<sub>2</sub> requirement as a mechanism for the containment of genetically modified cyanobacteria. *ACS Synth. Biol.* Epub Jan 10, 2018. DOI: 10.1021/acssynbio.7b00377.
49. **Moe-Behrens, G. G., Davis, R., and Haynes, K. A. (2013).** Preparing synthetic biology for the world. *Front. Microbiol.* 4, 5.
50. **Collier, J. L., and Grossman, A. R. (1992).** Chlorosis induced by nutrient deprivation in *Synechococcus* sp. strain PCC 7942: not all bleaching is the same. *J. Bacteriol.* 174, 4718-4726.

51. **Johnsborg, O., Eldholm, V., and Havarstein, L. S. (2007).** Natural genetic transformation: prevalence, mechanisms and function. *Res. Microbiol.* 158, 767-778.
52. **Draskovic, I., and Dubnau, D. (2005).** Biogenesis of a putative channel protein, ComEC, required for DNA uptake: membrane topology, oligomerization and formation of disulphide bonds. *Mol. Microbiol.* 55, 881-896.
53. **Stingl, K., Muller, S., Scheidgen-Kleyboldt, G., Clausen, M., and Maier, B. (2010).** Composite system mediates two-step DNA uptake into *Helicobacter pylori*. *Proc. Natl. Acad. Sci. U.S.A.* 107, 1184-1189.
54. **Schuergers, N., Ruppert, U., Watanabe, S., Nurnberg, D. J., Lochnit, G., Dienst, D., Mullineaux, C. W., and Wilde, A. (2014).** Binding of the RNA chaperone Hfq to the type IV pilus base is crucial for its function in *Synechocystis* sp. PCC 6803. *Mol. Microbiol.* 92, 840-852.
55. **Mu, D. Y., Min, M., Krohn, B., Mullins, K. A., Ruan, R., and Hill, J. (2014).** Life cycle environmental impacts of wastewater-based algal biofuels. *Environ Sci Technol* 48, 11696-11704.
56. **Mino, T., Van Loosdrecht, M. C. M., and Heijnen, J. J. (1998).** Microbiology and biochemistry of the enhanced biological phosphate removal process. *Water Res* 32, 3193-3207.
57. **Green, M. R., and Sambrook, J. (2012).** *Molecular cloning: a laboratory manual*. 4th ed., Cold Spring Harbor Laboratory Press, Cold Spring Harbor, New York.
58. **Neidhardt, F. C., Bloch, P. L., and Smith, D. F. (1974).** Culture medium for enterobacteria. *J. Bacteriol.* 119, 736-747.

59. **Rice, P., Longden, I., and Bleasby, A. (2000).** EMBOSS: The European molecular biology open software suite. *Trends Genet.* 16, 276-277.
60. **Bornscheuer, U. T., Huisman, G. W., Kazlauskas, R. J., Lutz, S., Moore, J. C., and Robins, K. (2012).** Engineering the third wave of biocatalysis. *Nature* 485, 185-194.
61. **Straathof, A. J. J. (2014).** Transformation of biomass into commodity chemicals using enzymes or cells. *Chem. Rev.* 114, 1871-1908.
62. **Wang, X., Saba, T., Yiu, H. H. P., Howe, R. F., Anderson, J. A., and Shi, J. (2017).** Cofactor NAD(P)H regeneration inspired by heterogeneous pathways. *Chem.* 2:621-654.
63. **Wandrey, C., Liese, A., and Kihumbu, D. (2000).** Industrial biocatalysis: past, present, and future. *Org. Process. Res. Dev.* 4, 286-290.
64. **Schmid, A., Dordick, J. S., Hauer, B., Kiener, A., Wubbolts, M., and Witholt, B. (2001).** Industrial biocatalysis today and tomorrow. *Nature* 409, 258-268.
65. **Woodyer, R., van der Donk, W. A., and Zhao, H. M. (2006).** Optimizing a biocatalyst for improved NAD(P)H regeneration: directed evolution of phosphite dehydrogenase. *Comb. Chem. High Throughput Screen* 9, 237- 245.
66. **Hollmann, F., Arends, I. W. C. E., and Buehler, K. (2010).** Biocatalytic redox reactions for organic synthesis: nonconventional regeneration methods. *Chem. Cat. Chem.* 2, 762-782.
67. **van der Donk, W. A., and Zhao, H. (2003).** Recent developments in pyridine nucleotide regeneration. *Current Opinion in Biotechnology* 14, 421-426.
68. **Faber, K. (2004).** Biotransformations in organic chemistry; 5th edition ed.; Springer Verlag: Berlin, Germany.

69. **Hummel, W., and Kula, M.-R. (1989).** Dehydrogenases for the synthesis of chiral compounds. *Eur J. Biochem.* 184, 1-13.
70. **Krix, G., Bommarius, A. S., Drauz, K., Kottenhahn, M., and Schwarm, M. (1997).** Enzymatic reduction of  $\alpha$ -keto acids leading to L-amino acids, D- or L-hydroxy acids. *Journal of Biotechnology* 53, 29-39.
71. **Wichmann, R., Wandrey, C., Buckmann, A. F., and Kula, M. R. (1981).** Continuous enzymatic transformation in an enzyme membrane reactor with simultaneous NAD(H) regeneration. *Biotechnol. Bioeng.* 67,791-804.
72. **Chenault, H. K., and Whitesides, G. M. (1987).** Regeneration of nicotinamide cofactors for use in organic synthesis. *Appl. Biochem. Biotechnol.* 14, 147-197.
73. **Wu, H., Tian, C., Song, X., Liu, C., Yang, D., and Jiang, Z. (2013).** Methods for the regeneration of nicotinamide coenzymes. *Green Chem.* 15, 1773.
74. **Wichmann, R., and Vasic-Racki, D. (2005).** Cofactor regeneration at the lab scale. *Adv. Biochem. Engin./Biotechnol.* 92, 225-260.
75. **Weckbecker, A., Groger, H., and Hummel, W. (2010).** Regeneration of nicotinamide coenzymes: principles and applications for the synthesis of chiral compounds. *Adv. Biochem. Eng. Biotechnol.* 120, 195-242.
76. **Tishkov, V. I., and Popov, V. O. (2006).** Protein engineering of formate dehydrogenase. *Biomolecular Engineering*, 23, 89-110.

77. **Seelbach, K., Riebel, B., Hummel, W., Kula, M.-R., Tishkov, V. I., Egorov, A. M., et al. (1996).** A novel, efficient regenerating method of NADPH using a new formate dehydrogenase. *Tetrahedron Letters* 37, 1377-1380.
78. **Rissom, S., Schwarz-Linek, U., Vogel, M., Tishkov, V. I., and Kragl, U. (1997).** Synthesis of chiral E-lactones in a two-enzyme system of cyclohexane monooxygenase and formate dehydrogenase with integrated bubble-free aeration. *Tetrahedron: Asymmetry* 8:2523-2526.
79. **Tishkov, V. I., Galkin, A. G., Fedorchuk, V. V., Savitsky, P. A., Rojkova, A. M., Gieren, H., et al. (1999).** Pilot scale production and isolation of recombinant NAD<sup>+</sup>- and NADP<sup>+</sup>-specific formate dehydrogenases. *Biotechnology and bioengineering* 64, 7.
80. **Vrtis, J. M., White, A. K., and Metcalf, W. W. (2002).** Phosphite dehydrogenase: a versatile cofactor-regeneration enzyme. *Angew. Chem. Int. Ed. Engl.* 41, 3257-3259.
81. **Relyea, H. A., and van der Donk, W. A. (2005).** Mechanism and applications of phosphite dehydrogenase. *Bioorg. Chem.* 33,171-189.
82. **Motomura, K., Sano, K., Watanabe, S., Kanbara, A., Abdel-Hady G. N., Ikeda, T., et al. (2018).** Synthetic phosphorus metabolic pathway for biosafety and contamination management of cyanobacterial cultivation. *ACS Synth. Biol.* 7, 2189-2198.
83. **Johannes, T. W., Woodyer, R. D., and Zhao, H. (2005).** Directed evolution of a thermostable phosphite dehydrogenase for NAD(P)H regeneration. *Appl. Environ. Microbiol.* 71, 5728-5734.
84. **Woodyer, R., van der Donk, W. A., and Zhao, H. (2003).** Relaxing the nicotinamide cofactor specificity of phosphite dehydrogenase by rational design. *Biochemistry* 42, 11604-11614.

85. **Johannes, T. W., Woodyer, R. D., and Zhao, H. (2007).** Efficient regeneration of NADPH using an engineered phosphite dehydrogenase. *Biotechnol. Bioeng.* 96, 18-26.
86. **Sambrook, J., Fritsch, E. F., and Maniatis, T. (1989).** Molecular cloning: a laboratory manual, 2nd ed. Cold Spring Harbor Laboratory Press, Cold Spring Harbor, NY.
87. **Yokoyama, S., Matsuo, Y., Hirota, H., Kigawa, T., Shirouzu, M., Kuroda, Y., et al. (2000).** Structural genomics projects in Japan. *Progress in Biophysics and Molecular Biology* 73, 363-376.
88. **Carugo, O., and Argos, P. (1997).** NADP-dependent enzymes. I: conserved stereochemistry of cofactor binding. *Proteins Struct. Funct. Genet.* 28, 10-20.
89. **Petschacher, B., Staunig, N., Müller, M., Schürmann, M., Mink, D., De Wildeman, S., et al. (2014).** Cofactor specificity engineering of *streptococcus* mutants NADH oxidase 2 for NAD(P) regeneration in biocatalytic oxidations. *Computational and Structural Biotechnology Journal* 9, e201402005
90. **Chánique, A. M., and Parra, L. P. (2018).** Protein engineering for nicotinamide coenzyme specificity in oxidoreductases: attempts and challenges. *Front. Microbiol.* 9, 194.
91. **Ghosh, S., Mohan, U., and Banerjee, U. C. (2016).** Studies on the production of shikimic acid using the aroK knockout strain of *Bacillus megaterium*. *World J. Microbiol. Biotechnol.* 32, 127.
92. **Liu, Y., Feng, Y., Wang, L., Guo, X., Liu, W., Li, Q., et al. (2019).** Structural insights into phosphite dehydrogenase variants favoring a non-natural redox cofactor. *ACS Catal.* 9, 1883-1887.
93. **Wojciechowski, M., and Lesyng, B. (2004).** Generalized born model: analysis, refinement, and applications to proteins. *J. Phys. Chem. B* 108, 18368-18376.

94. **Labute, P. (2008).** The generalized Born/volume integral implicit solvent model: estimation of the free energy of hydration using London dispersion instead of atomic surface area. *J. Comput. Chem.* 29, 1693-1698.
95. **Zhang, L., Ahvazi, B., Szittner, R., Vrieling, A., and Meighen, E. (1999).** Change of nucleotide specificity and enhancement of catalytic efficiency in single point mutants of *Vibrio harveyi* aldehyde dehydrogenase. *Biochemistry* 38, 11440-11447.
96. **Corbier, C., Clermont, S., Billard, P., Skarzynski, T., Branlant, C., Wonacott, A., et al. (1990).** Probing the coenzyme specificity of glyceraldehyde-3-phosphate dehydrogenases by site-directed mutagenesis. *Biochemistry* 29, 7101-7106.
97. **Fukada, H., Sturtevant, J., and Quioco, F. (1983).** Thermodynamics of the binding of L-arabinose and of D-galactose to the L-arabinose-binding protein of *Escherichia coli*. *J. Biol. Chem.* 258: 13193-13198.
98. **Brandts, J. F., and Lin, L. N. (1990).** Study of strong to ultratight protein interactions using differential scanning calorimetry. *Biochemistry* 29, 6927-6940.
99. **Shrake, A., and Ross, P. D. (1990).** Ligand-induced biphasic protein denaturation. *J. Biol. Chem.* 265, 5055-5059.
100. **Doukyu, N., and Ogino, H. (2010).** Organic solvent-tolerant enzymes. *Biochemical Engineering Journal* 48, 270-282.
101. **Jiang, H.-W., Chen, Q., Pan, J., Zheng, G.-W., and Xu, J.-H. (2020).** Rational engineering of formate dehydrogenase substrate/cofactor affinity for better performance in NADPH regeneration. *Appl. Biochem. Biotechnol.* 192, 530-543.

102. **Calzadiaz-Ramirez, L., Calvó-Tusell, C., Stoffel, G. M. M., Lindner, S. N., Osuna, S., Erb, T. J., et al. (2020).** *In vivo* selection for formate dehydrogenases with high efficiency and specificity toward NADP. *ACS Catal.* 10, 7512-7525.
103. **Serov, A. E., Popova, A. S., Fedorchuk, V. V., and Tishkov, V. I. (2002).** Engineering of coenzyme specificity of formate dehydrogenase from *Saccharomyces cerevisiae*. *Biochemical Journal* 367, 841-847.
104. **Tamoi, M., Miyazaki, T., Fukamizo T., and Shigeoka, S. (2005).** The Calvin cycle in cyanobacteria is regulated by CP12 via the NAD(H)/NADP(H) ratio under light/dark conditions. *The Plant Journal.* 42, 504-513.

## **Acknowledgments**

Praise be to Allah, his majesty for his uncountable blessings, and best prayers and peace be upon the Prophet Mohamed the most beloved Prophet of Allah, his relatives, and noble companions.

I would like to express my sincere gratitude to my academic advisor Dr. Ryuichi Hirota, Associate Professor of the Department of Molecular Biotechnology, Graduate School of Integrated Sciences for Life, Hiroshima University, for his instruction and continuous encouragement throughout this study., as well as his experimental guidance.

I would like to express my deep appreciation to Dr. Akio Kuroda, professor of the Department of Molecular Biotechnology, Graduate School of Integrated Sciences for Life, Hiroshima University, for his kind instruction, scientific guidance, and encouragement throughout this study.

I would like to thank Dr. Junichi Kato and Dr. Yutaka Nakashimada, Professors of the Department of Molecular Biotechnology, Graduate School of Integrated Sciences for Life, Hiroshima University, for their precious advice and the review of this thesis.

I also thank Dr. Hisakage Funabashi, Dr. Takashi Ikida, Associate Professors, and Dr. Takenori Ishida, Assistant Professors of the Department of Molecular Biotechnology, Graduate School of Integrated Sciences for Life, Hiroshima University, for valuable discussions throughout this study.

Many thanks go to Dr. Hiroki Murakami, Mr. Tomoki Nishimura, researchers of Kuroda Lab and Ms. Takako Sawahara, the secretary of Kuroda Lab, for their support.

I would like to thank my colleagues, graduate, and undergraduate students of Kuroda Lab for their kind help and support.

I would like to thank my parents, my wife, and my beloved sons and daughter, for their continuous encouragement and support.

Lastly, I would like to thank my government, Egypt, in particular the Ministry of Higher Education and Scientific Research for honoring me and funding me to conduct this research in Japan. My thanks are also for my professors and colleagues of the Department of Genetics, Faculty of Agriculture, Minia University, Egypt, for their continued support.

*Gamal N. Abdelhady*

## Articles

- 1) Synthetic phosphorus metabolic pathway for biosafety and contamination management of cyanobacterial cultivation.

Kei Motomura, Kosuke Sano, Satoru Watanabe, Akihiro Kanbara, Gamal Nasser Abdel-Hady, Takeshi Ikeda, Takenori Ishida, Hisakage Funabashi, Akio Kuroda, and Ryuichi Hirota.

ACS Synthetic Biology, 7, 2189-2198 (2018).

- 2) Engineering cofactor specificity of a thermostable phosphite dehydrogenase for a highly efficient and robust NADPH regeneration system.

Gamal Nasser Abdel-Hady, Takeshi Ikeda, Takenori Ishida, Hisakage Funabashi, Akio Kuroda, and Ryuichi Hirota.

Frontiers in Bioengineering and. Biotechnology, 9, 647176 (2021).